New Naphthalene Diimide Dye Synthesis Containing Powerful Binding Sites for Metal Ions

Hengameh Jowzaghi

Submitted to the
Institute of Graduate Studies and Research
in partial fulfillment of the requirements for the degree of

Master of Science
in
Chemistry

Eastern Mediterranean University
September 2016
Gazimağusa, North Cyprus

Approval of the Institute of Graduate Studies and Research

Prof. Dr. Mustafa Tümer
Acting Director

I certify that this thesis satisfies the requirements as a thesis for the degree of Master of Science in Chemistry.

Prof. Dr. Mustafa Halilsoy
Chair, Department of chemistry

We certify that we have read this thesis and that in our opinion, it is fully adequate in scope and quality as a thesis for the degree of Master of Science in Chemistry.

Prof. Dr. Huriye İcil
Supervisor

Examining Committee

1. Prof. Dr. Huriye İcil
2. Asst. Prof. Dr. Süleyman Aşır
3. Asst. Prof. Dr. Nur P. Aydınl

ABSTRACT

Naphthalene diimides (NDI) are a class of organic dyes with optical, thermal, and photochemical properties and stability. Hence, its importance in the rapidly developing modern technology, have found expression amongst researchers.

NDI interaction with metals is expected to make change in photophysical and photochemical properties of sensitizers such as wavelength shifts and intensity changes in absorption and emission spectra. Consequently, metal complexation of NDI leads to high potential towards organic electronic application.

The synthesized compound exhibit different intermolecular interactions in different solvents which enhances its utilization in photonic and optoelectronic application.

Therefore, this project aims to synthesize a new NDI dye containing powerful binding site for metal ions. By condensation reaction, NDA and an amine (4,6-diamino-2-pyrimidine-thiol) reacts with isoquinoline and m-cresol solvent mixture in the presence of argon gas. The synthesized product was investigated by IR and UV-vis spectroscopy, TGA and DSC analysis for thermal behavior and elemental analysis.

Keywords: Naphthalene diimides.

ÖZ

Naftalin diimidler (NDI), optik, ve fotokimyasal özellikleri ve termal kararlılıkları ile bilinen organik boya sınıfındandırlar. Bu nedenle, hızla gelişen modern teknolojide yer almışlar ve araştırmacıların ilgi noktası olmuşlardır.

NDI-metal etkileşimi absorpsiyon ve emisyon spektrumları, dalga boyu değişiklikleri gibi fotofiziksel ve fotokimyasal özellikleri de değişiklik yapmabilmektedir. Sonuç olarak, NDI metal kompleksleşmesi organik elektronik uygulamalarına uygun potansiyele sahiptir.

Sentezlenmiş bir bileşik değişik çözgenlerde farklı moleküller arası ilişkiler ile fotonik ve optoelektronik özellikleri geliştirir.

Bu nedenle, bu proje metal iyonları için güçlü bağlanma bölgesini içeren yeni bir NDI boya sentezlemek amaçlamaktadır. Kondensasyon reaksiyonu, NDA ve bir amin (4,6-diamino-2-pirimidin-tiyol) ile, argon gazı varlığında izokinolin ve m-kresol çözgen karışımında reaksiyona girer. Sentezlenen ürün IR ve UV-vis spektroskopisi ve TGA ve DSC analizi ile karakterize edilmiştir.

Anahtar Kelimeler: Naftalin diimidler.

To My Prof.Dr.H.Icil

ACKNOWLEDGMENT

I would like to express my deep appreciation to my supervisor **Prof. Dr. Huriye İcil** for her inspiration and guidance throughout this work. This thesis would not have been possible without her support.

I would also like to thank the examining committee members Prof. Dr. Huriye İcil, Asst. Prof. Dr. Nur P. Aydınlık, Asst. Prof. Dr. Süleyman Aşır for taking time to review my thesis.

Last, but not least, I would like to thank all of the group members of İcil's Organic Group, specially Basma Al-Khateeb and Dr. Duygu Uzun for all the learning moments and good times that we shared in and out of the lab.

I want to express my sincerest gratitude to my family for their support, unending love and patience during my study.

I would also like to thanks to other staff members of the Department of Art and Science of Eastern Mediterranean University for their helps.

TABLE OF CONTENTS

LIST OF TABLES

LIST OF FIGURES

LIST OF ILLUSTRATIONS

LIST OF ABBREVIATIONS

A°	Armstrong
A	Absorbance
C	Concentration
C°	Degree Celsius
DMSO	Dimethyl Sulfoxide
DCM	Dichloromethane
λ_{exc}	Excitation Wavelength
K_f	Fluorescence Rate Constant
τ_f	Fluorescence Lifetime
FT – IR	Fourier Transform Infrared Spectroscopy
$\Delta\bar{\upsilon}_{1/2}$	Half-width of the Selected Absorption
IR	Infrared Spectroscopy
ε	Molar Absorption Coefficient
λ_{max}	Maximum Absorption Wavelength
M	Molar Concentration
Min	Minute
Mmol	Millimole
ε_{max}	Maximum Extinction Coefficient
NDI	Naphthalene diimide
NDA	Naphthalene 1,4,5,8-tetracarboxylic dianhydride

NMP	N-Methylpyrrolidone
DMF	N, N’-dimethylformamide
F	Oscillator Strength
KBr	Potassium Bromide
k_d	Rate Constant of Radiationless Deactivation
E_s	Singlet Energy
TGA	Thermogravimetric Analysis
TCE	Trichloroethylene
TFA	Trifluoroacetic Acid
τ_0	Theoretical Radiative lifetime
UV-vis	Ultraviolet Visible Absorption Spectroscopy
Hb	Hydrogen bond
ET	Electron Treansfer
EET	Electronic Energy Transfer
RET	Resonance Energy Transfer

Chapter 1

INTRODUCTION

1.1 Naphthalene Diimide

The naphthalene diimide (NDI) is the smallest possible co-compound among the broader category of compounds called rylene diimides, (RDI). The RDIs are industrial dyes and pigments groups with naphthalene units linked together in enclosed positions [1].

The naphthalene diimides (NDIs) are likewise known as naphthalene carbodiimides or 1,4,5,8-Naphthalenediimides (Figure 1.1) possess fluorescent properties, and are chemically robust, inert, stable, redox-active synthesis of high melting points. Vollmann et al. (2006) reported the most pioneering investigation of the physiochemical properties of NDI and its varieties in the early 1930s, which led to the substantial demand of their study towards the latter end of the 20th century and even until recent times [2].

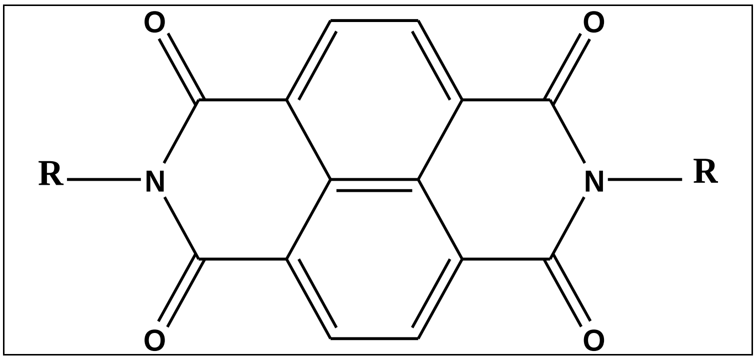

Figure 1.1: General structure of naphthalene diimide

The basic structure of NDI compound consists of a naphthalene core that possesses two annulated electrons-withdrawing imide carbonyl groups at its four α-positions. The NDIs rigid structure consists of strong intermolecular π-π interaction and π-conjugated heterocyclic family. The nitrogen atom in NDIs has a propensity to be replaced with a kind of alkyl or aryl by-products [3-4].

Naphthalene diimides are compact, a deficient electron group of aromatic compound capable of self-configuration and self-incorporation into bigger multi compound groups via intercalation. The NDI has distinct properties of the smaller aromatic core, colorless solids of high purity with UV irradiation absorption ability in aqueous solution [5].

NDIs find applications in the production of conducting materials and have drawn much focus due to their ability to produce n-type rather than p-type semiconductor products [6].

The NDI has attracted significant interest among researchers because of its thermal stability, excellent electron acceptor properties, and high level of solubility in aqueous solution [7].

In the last few decades, it was proven that perylene diimide is the most important among the rylene diimides, RDI. In spite of this, the active redox properties of NDI, its substitution of naphthalene core and its replacement with aromatic functional groups makes NDI have better spectrum- structural and photophysical properties [8].

Also, the NDIs have fabrication and functional properties than their main unsubstituted counterparts, such as pyromellitic diimides and perylene diimide. The NDI electronic properties have a tendency to improve by applying substitutes at either the naphthalene core or the N atom of the amide groups [9].

Due to NDIs core, which contains naphthalene rings, they are applicable in organic, optical, photovoltaic and semiconductor devices with high optical absorption and magnitude of charge transport due to NDIs bright colored and conducting properties (Icil H, Ozser M 2013).

Naphthalene diimides are essential components for the production of functional supramolecular materials, used as organic field effect transistors, molecular switches, sensors and also extends to biological and medical applications [10].

Further applications of NDI are found in the photolysis of NDI to reduce heme proteins , photoactivation of hydroperoxy to oxidize both proteins and, DNA [11], etc.

The substitution of diimide nitrogen in the primary NDI is used as electron acceptors, to serve as a building framework for fragmentary charge transfer stabilization and form a new molecular or supermolecular array of compounds [12].

The quality of color and fluorescence of core substituted describe the quality of the NDIs. Hence, little effect is necessary for structure for absorbing through the entire visible spectra of NDIs [13].

One of the applications and the significant use of NDIs are to improve drug industry. One of such significance of NDIs is to establish active G-quadruplex-binding ligands. The production of a high cellular anti-toxicity to improving G-quadruplex DNA specific structure and appropriate binding ligands are the primary involvement in drug, cancer studies, and therapeutic, design application and usability research studies [14].

1.2 Hydrogen Bond Donor

The hydrogen bond (Hb) donor is a molecule that supplies the hydrogen atom of a hydrogen bond to a relatively electromagnetic atom such as fluorine (F), nitrogen (N), and oxygen (O). There must be both an H-donor and an acceptor present for Hb to occur.

The hydrogen bonding between some heavy molecular compounds and NDIs, coupled with noncovalent interactions such as aromatic-aromatic, electrostatics, etc. are responsible for the formation of supramolecular arrays of different compounds [15].

Sessler et al. (1998) proposed the synthesis of the first rigid, coplanar electron-donor framework system using hydrogen bonding. In their study, a novel donor (porphyrin) and an acceptor (NDI) were present. The Hb between the diimide and a 2, 6-diaminopyridine produced the supramolecular arrays of triple point hydrogen bonded dyad [16].

Also, the Hb between carboxylic acid ends linked with the hydrophobic spots within the NDI inner cores is majorly attributed to the production of such supramolecular design of such naphthalene diimides possessing carboxylic acid compound groups (Figure 1.2) (Bhosale S, Jani H 2007).

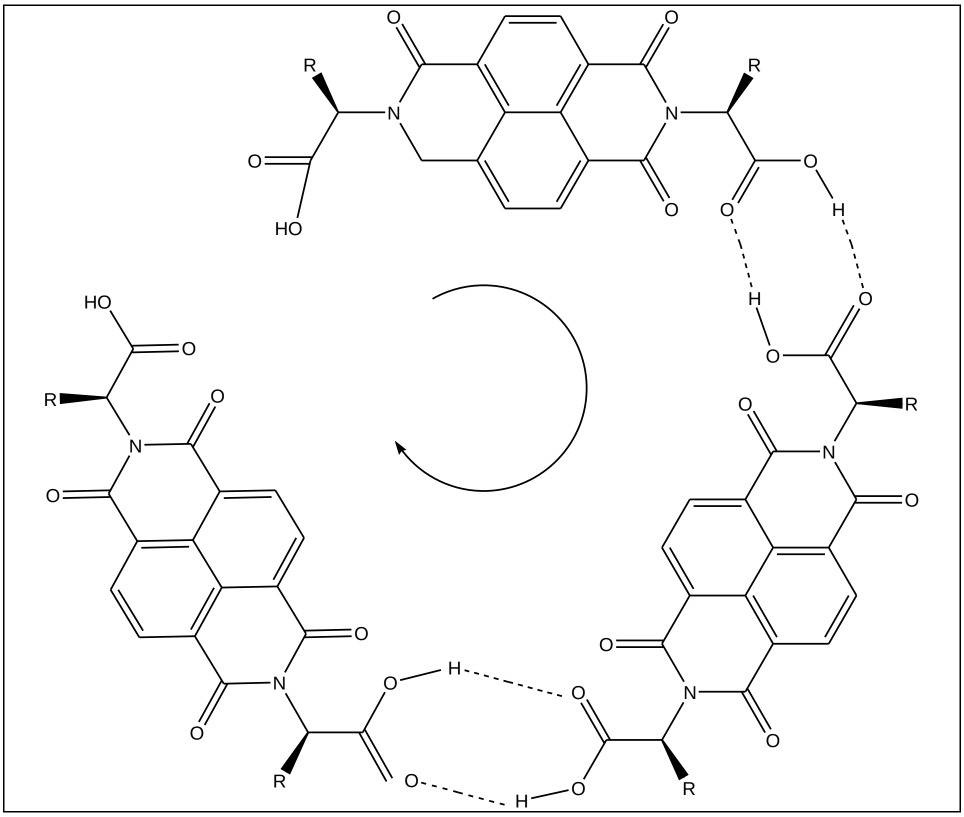

Figure 1.2: The helical kind of a chiral NDI dicarboxylic acid array forms hydrogen-bonded organic nanotubes in aqueous solution and the solid state.

The systematic donor–acceptor synthesis, organic scaffolds and well-arranged supramolecular systems have been formed through selective functionalization of NDIs for the formation of useful characteristic compounds, with broad applications and functions.

The hydrogen bonding in supramolecular chemistry of intermolecular amide-amide assembly enhances the fabrication of well-organized arrays and has initiated new functional electronic products. The synthesis of self-assembled nanostructures, helical nanorods, nanotube biomaterials and polymers and all forms of aggregation-induced supramolecular NDIs derivates can be initiated by Hb [17]. Therefore, the functionalization and characteristics of hydrogen bonding have potential applications to develop more supramolecular systems and compounds in the future.

1.3 Self-Assembly of Naphthalene Diimide

Self-assembly **(SA)** is a systematic process through which disorganized systems of pre-existing components synthsize themselves into a well-organized pattern or structure spontaneously via interaction. This interaction could be as a result of precise, local reactions among the materials themselves, without external direction to produce a larger functional unit. The spontaneous arrangement can be due to direct distinct interaction and, or indirectly through their immediate environment.

The phenomenon application of nanotechnology to self-assembled nanoparticles that can be potentially used to produce increasingly sophisticated structures forming a broad range of materials used for different purposes. When the constituent components are molecules, it is termed a molecular self-assembly. It could either be static or dynamic.

Biological systems rely on the power of self-assembly to build incredible, precise and complex supramolecular arrays from assemblies of small building units, for example, the double helix of DNA. Different nanotechnological concepts have been used to mimic the mode of assembly and structures of biological systems to build variety of self-organized compounds from abiotic arrays into fibers, layers, tubes, etc.

Such phenomenon finds application in self-assembly, p-conjugated elements such as ambipolar dipolar or systems, the liquid-crystalline mesogens, organic semi-conductors [18]. A promising n-type semiconductor such as Naphthalenediimide (NDI) finds application in the synthesis of a broad range of ordered structural compounds in solution (Figure 1.3). In the time past, researchers have been engrossed in studying the supramolecular array of NDI derivatives by proper understanding of

H-bonding that functions along a specified direction within the NDIs core, a strategy that has been used to synthesize other useful compounds [19].

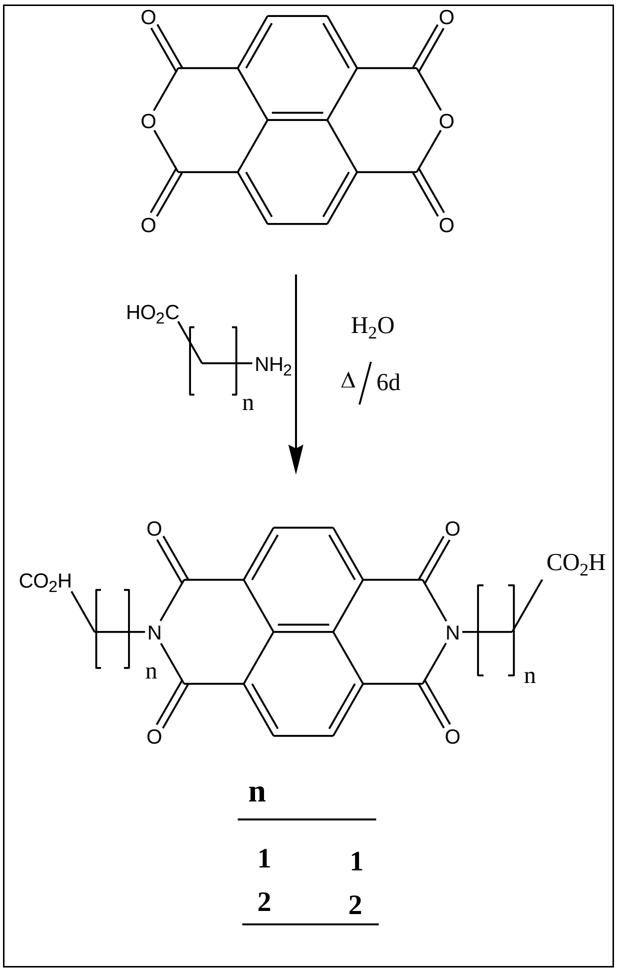

Figure 1.3: Synthesis of the naphthalene diimides 1 and 2 [20].

Therefore, this thesis aims to synthesize a new NDI compound using the hydrogen bonding and self-assembly phenomena. The synthetic product is characterized by DSC, FTIR, TGA, UV-Vis, emission and elemental analysis.

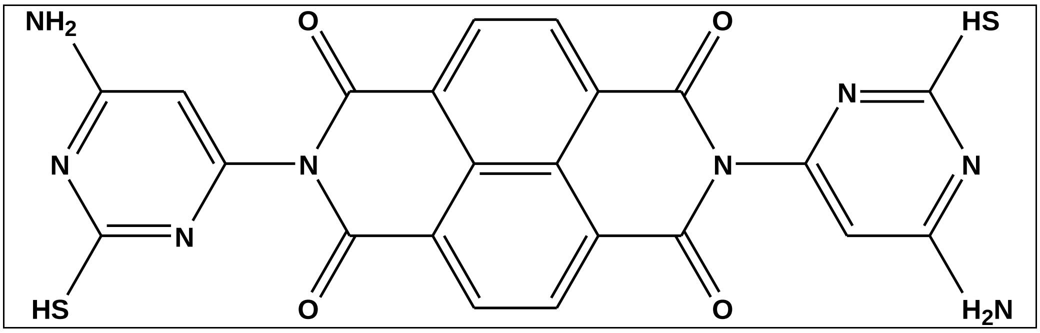

Figure 1.4: Structure of TNDI

Chapter 2

THEORETICAL

2.1 Synthesis And Applications of Naphthalene Diimide

Naphthalene diimides, NDIs are the smallest homologues of the perylene diimides and they are synthesized from the dianhydride compounds. NDIs are the low to high weighty organic supramolecular semiconductor components among the n-type compounds with favorable electrochemical and photophysical properties and fluorescence quantum yield.

In recent years, the primary synthesis studies were examined to facilitate the structural modifications of the naphthalene diimides. The NDI compounds possess electrical, optical, photochemical and photosynthetic properties that are easily and more efficiently subjected to core functionalization through relatively little synthetic effort. The synthesis of NDI occurs via a suitable imide and/or core substitution (2,6- or 2,3,6,7- to the core) yielding a kind whose absorption and fluorescence properties are different [21].

The electron-deficient properties of NDIs make them highly valuable materials, most especially in the field of organic electronics as air-resistant to air-stable n-type semiconductors. The NDIs ability to absorb different bands of the visible spectral range in the core substituents produces photosystems and photovoltaic properties [22]. The NDIs organic electronic synthesis is semiconductors which possess numerous advantages, such as flexible components that are cheap of low-temperature processability, large specific coated area, etc. [23]. Also, the NDIs possess air stability, excellent oxidative stability, high electron affinities, high electron mobilities, optoelectronic tunability, photochemical stability, thermal, and finally good light absorption characteristics [24-25].

These properties of NDIs organic molecules make them a top active part of a broad range of organic diodes, organic field-conductive transistors, organic photovoltaic cells and non-volatile memory devices [26]. Two major methods can achieve the chemical modification of the NDIs. Firstly, is to introduce the substituents at the N atoms of imide groups and this has a little effect on the electrochemical and optical properties of NDI components. Though the N, N’ substituents of NDIs can be used to control the aggregation, intermolecular packing and solubility in their stable states.

Figure 2.1 represents the schematic diagram of the synthetic paths to naphthalene imides 1-7. The synthesised NDIs have lots of applications because of their different properties such as brilliant colour, high absorption and fluorescence, and excellent electrochemical and photochemical stability (Gudeika D, Lygaitis R 2012).

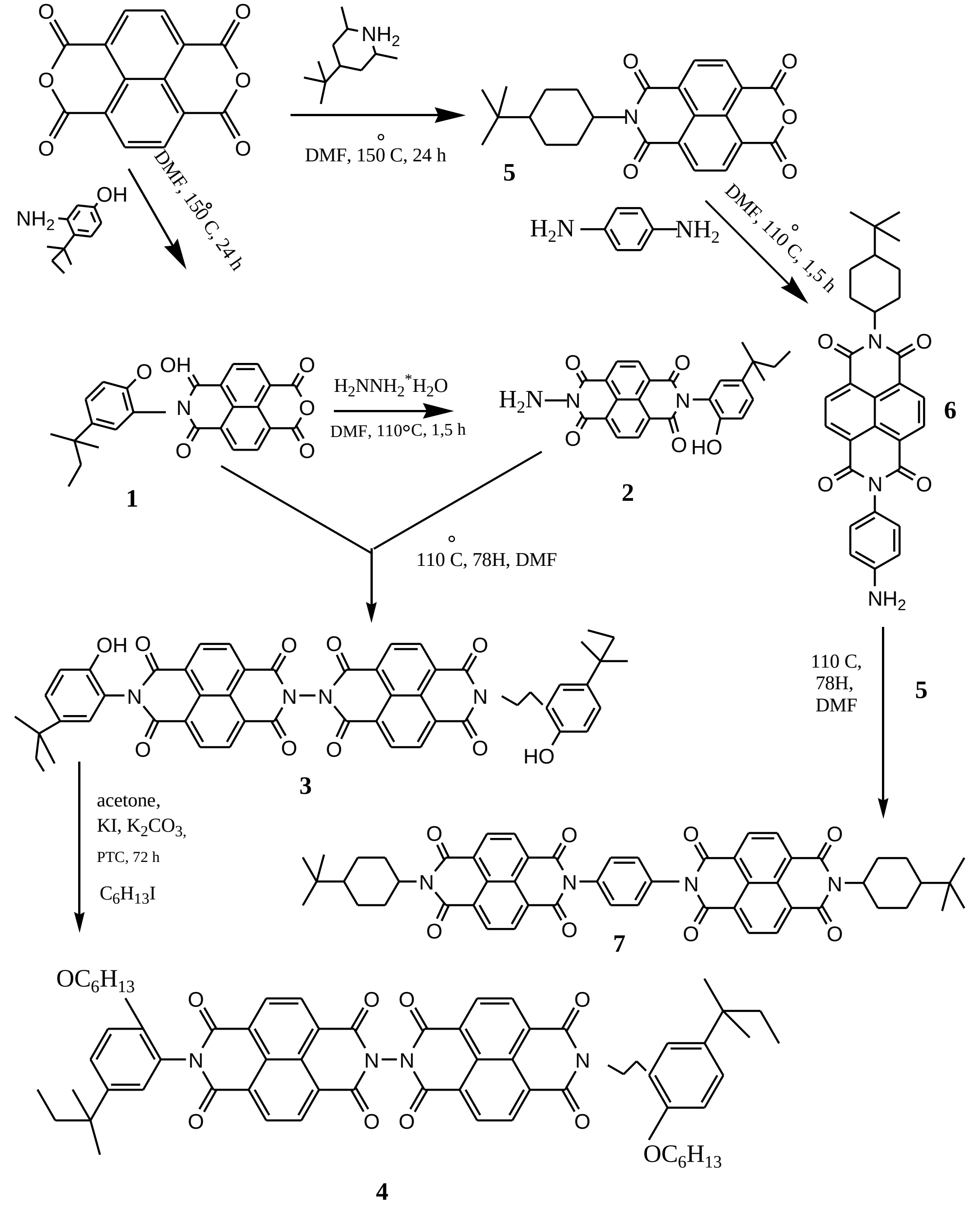

Figure 2.1: Synthetic routes to naphthalene imides 1–7

The second approach is by functionalization of core substituted NDIs which have a much more remarkable effect on the optical spectra and redox potentials [27-28]. Thus, the compounds have weak absorption strength for visible light, limiting their possibilities for optoelectronic applications. The literature review comprises the examination of the NDIs syntheses by several researchers using different methods and chemical species.

Gudeika et al. (2012) in their study synthesized the dimeric naphthalene diimide compounds through the condensation of a 1,4,5,8-naphthalene-tetracarboxylic dianhydride with different aromatic amines such as 2-amino-4-tert-amylphenol and 4-tert-butylcyclohexylamine. Also, in using linking agents such as hydrazine and p-phenylenediamine. Figure 2.2 shows the synthesis paths and characterization for new monomers of NDIs, an electrochemical and optical studies performed by Ghadah (2014).

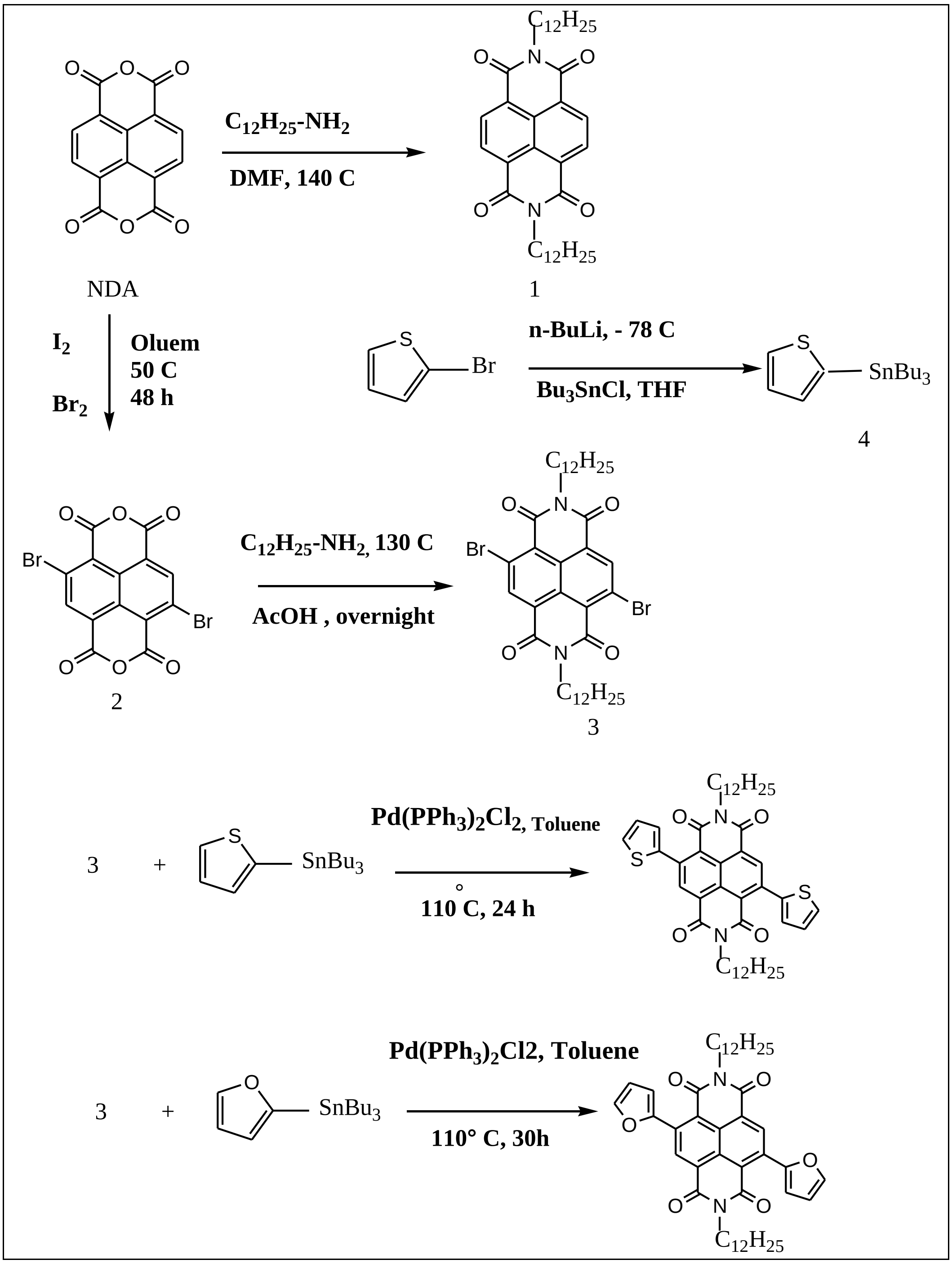

Figure 2.2: Systematic routes of monomers [29]

The literature review has reported many derivatives of NDIs have significant properties suitable for a broad range of biotechnological applications, molecular devices and optical and photonic materials.

Biotechnology comprises a wide variety of genetic engineering application that covers entire conventional procedures for modifying living organisms. For example, it is applicable in native plants to improve food productions in meeting the human needs through artificial selection and hybridization. The NDIs also use in a wide-ranging of biotechnological applications. They play role as a high quality electron acceptors and the photolysis of NDIs decreases heme proteins. Furthermore, the derivatives of NDIs are used for duplex DNA intercalation, to oxidise protein-DNA, for triplexes and stabilisation of DNA hairpins, etc. [30].

The NDIs find application in a molecular-level component for detecting the discrete number of a supramolecular structure designed to initiate a particular function. Finally, the uses of NDIs are prominent in the optical and photonic materials, machines or devices [31].

The optical and photo-electronic devices contribute an important role in the systematic electrical components and telecommunication devices and systems. Photonics is the scientific platform to control, detect and generate the electromagnetic spectrum from 0.2 to 12 μm wavelength. The photonic devices comprise optoelectronic devices such as lasers, optical fibre, planar photodetectors and waveguides-based passive devices [32].

The NDIs finds application in organic photo-refractive compounds for electron migrating constituents in fluorescent dyes, organic light-discharging diodes, optical signal processing, near-IR dyes and semiconducting materials for solar energy conversion [33].

2.2 Electron Transfer

The electron transfer (ET) is the transfer mechanism of the electron from an atom or molecule to another such entity. The category of ET reactions are the most fundamental of all chemical reactions and play an elemental role in many applications including amperometric sensors, biological methods, energy storage components, organic synthesis, etc. In recent times, molecular biological fields have attracted considerable attention in the study of electron transfer [34].

The different types of chemical reactions such as electrochemistry (an electrode), photochemistry, or an electron donor (reducing) or acceptor (oxidising) compounds initiate ET from one atom or molecule to another atom or molecule.

Michael Faraday (1843) experimented the first electro-organic synthesis. It was the anodic decarboxylation of acetic acid in an aqueous medium, and the formation of ethane compound via the creation of a new carbon-carbon bond.

$$2\ CH_3COO^- \xrightarrow[\text{pt}]{\text{-2e-}} CH_3CH_3 + 2CO_2 \qquad \text{(Eq. 2.1)}$$

Henry Kolbe (1849) performed electrolytic reactions on fatty acids and half-esters compounds of dicarboxylic acids and established the practical basis of electro-organic synthesis applications. At the beginning of the 20th century, different electrolytic industrial techniques emerged, mostly reductive in nature. These simulation of the techniques are the pioneering works of Kolbe, Haber, Fitcher, Tafel and other notable researchers who expanded the foundation of organic electrochemical, electroanalytical and spectra analytical methodologies [35-36].

The electron transfer can be initiated by the reduction of a functional group, such as hydrogenation of multiple C-C bonds. This reaction could be an indirect, electrocatalytic transfer, or a direct electron transfer to the multiple bonds as represented in Figure 2.3.

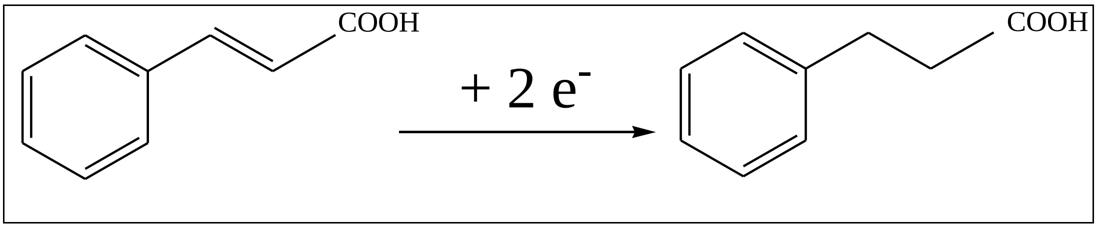

Figure 2.3: The electron transfer reduction of functional group

Also, the photoinduced ET process in the branch of photochemistry employs individual photoexcited molecules to behave as strong oxidizing or reducing species. Thus, induce a permanent chemical alteration in a ground state molecular ET mechanism. Figure 2.4 presents the illustration of the ground state redox reaction, where there is an electron transfer from a donor to an acceptor molecule [37].

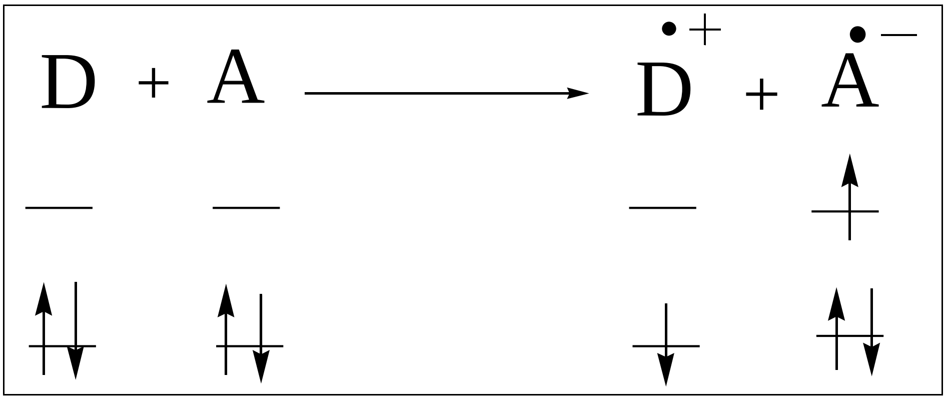

Figure 2.4: Ground state redox reactions

In the ground state, the free energy change in the ET process is the difference in the redox potentials of the donor and acceptor. Because of the large HOMO-LUMO gap in the ground state of organic molecules, ET would be a broad endothermic process. In addition to a donor (D) and an acceptor (A), photoinitiated ET reactions, photoelectron transfer requires an electronic excitation source (light) to occur [38].

2.3 Energy Transfer

The transfer mechanism between an excited electronic state of the emission of the light-sensitive molecule(s) (donor chromophore) to the absorption of an equivalent excited acceptor molecule (acceptor chromophore) is known as energy transfer (ET) or electronic energy transfer (EET) or resonance energy transfer (RET).

The donor molecule, in its initial electronic excited state, may transfer energy to an acceptor molecule through dipolar coupling mechanism. This mechanism occurs in two distinct ways. Firstly, it occurs through a nonradioactive fashion in a simple long-range dipolar coupling interactive system, in which an acceptor molecule absorbs a virtual photon emitted by an excited donor molecule. The nonradiative energy transfer occurs between a donor molecule and acceptor molecule, with both of them having a similar resonance frequency. The equations provided below illustrates the transfer concept:

$D + h\upsilon \rightarrow D^*$ (Eq. 2.2)

$D^* + A \rightarrow \mathrm{D} + \mathrm{A}^*$ ($D \rightarrow$ donor, $A \rightarrow$ Acceptor) (Eq. 2.3)

$A^* \rightarrow A + h\upsilon'$ (Eq. 2.4)

In contrast, the radioactive intermolecular interactions involve the radioactive energy transfer from the emission and reabsorption of a portion. This mechanism depends on the optical properties, physical dimensions of the specimen, the geometry of the medium and their wavefront pathways. Unlike radiative mechanisms, electronic energy transfer can produce a remarkable amount of structural information about the donor-acceptor pair. The Förster equation presents the rate constant of energy transfer:

$$k_{en} = \frac{0.592k^2\Phi_D J}{n^4 N\tau_D R^6} \qquad \text{(Eq. 2.5)}$$

k = the orientational factor,

Φ_D = the quantum yield of the fluorescence of the donor,

J = the overlap integral,

n = the dielectric constant of the medium.

Then, N = the Avogadro's number,

τ_D = the excited state of the lifetime of the donor molecule in the absence of energy transfer and R = the distance between the chromophores.

The electronic energy transfer mechanism between two molecular elements are the summation of two phenomena, coulombic and exchange. The two terms are dependent on different variables, and each of them is domineering based on the experimental and particular system's condition. The efficiency and rate at which any system occurs solely depend on the type of donor-acceptor pair, the kind of energy transfer, the spin nature of the net energy transfer, the distance of the donor-acceptor pair separation and the availability of molecular diffusion and/or energy migration.

As regards the coulombic mechanism, which is also reffered as dipole-dipole, Förster type mechanism or resonance, it takes a long range, which occurs via a ‘‘vacuum medium’’, that is, does not involve any physical contact (that is, interchange interaction) between the acceptor and the donor. The most versatile concept in this phenomenon is the coulombic dipolar transfer of two species, that is, the excitation of a dipole oscillation in A by D* as provided in equation 2.2 above. This example can be found in the large aromatic molecules of Naphthalene diimides. The so-called coluombic energy transfer is believed to have significant efficiency in which the radiative transfer connects the excited states of each molecule and ground to produce a high oscillation.

To compare the rate constant of resonance energy change with the photophysical and spectroscopic properties of the bi-molecular species, we require to evaluate another classical theory for Förster equation, by,

$$k_{en} = 1.25 \times 10^{17} \frac{\Phi_D}{n^4 \tau_D r_{DA}^6} \int_0^\infty F_D\,(\bar{\upsilon}) \varepsilon_A \frac{d\bar{\upsilon}}{\bar{\upsilon}^4} \qquad \text{(Eq. 2.6)}$$

Where ;

Φ_D, is the quantum produce of the donor emission, and n is the solvent refractive-index, τ_D is the life-span of the donor emission, r_{DA} is the nm-distance between acceptor and donor. Also, F_D is the emission spectrum of the donors (in normalized to unity and wave numbers) and ε_A is the decadic molar-extinction coefficient of the acceptor.

At short exchange distances, the Dexter-type exchange mechanism is usually considered. This mechanism requires the finite orbital overlap between the donor and acceptor pair. Conclusively, we have identified two major energy transfer routes, labeled the coulomb or resonance and the interchange energy transfer mechanism. Both of them are diagramatically represented in Figure 2.5.

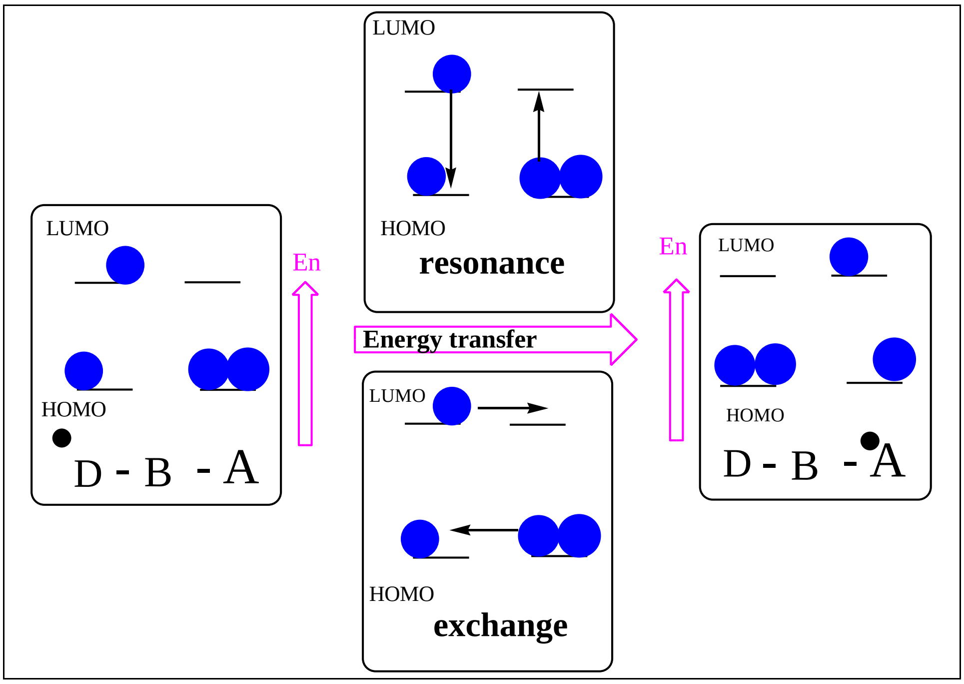

Figure 2.5: Pictorial representation of coulombic (resonance) and exchange energy transfer mechanisms [39].

Chapter 3

EXPERIMENTAL

3.1 Materials

1,4,5,8-Naphthaleneteteracarboxylic dianhydride (NDA), 4,6-diamino-2-prymidinethiol, zinc acetate, acetone, m-cresol and isoquinoline were purchased from Sigma Aldrich company and used without further purifications. High boiling point solvents were dried over molecular sieves (4-8 mesh) before use. Spectroscopic grade solvents were used for all spectroscopic analysis. Thin Layer Chromatography (TLC, aluminium sheets of 5 × 10 cm silica gel 60 F_{254}) used in order to control the progress of the synthesis and visualized by UV light.

3.2 Instruments

Ultraviolet absorption spectra in solutions were recorded by using Varian-Cary 100 Spectrophotometer. Infrared spectra were recorded by JASCO FT/IR-6200 spectrophotometer. In order to record the emission spectra Varian Cary Eclipse Fluorescence spectrophotometer was used.

Elemental analysis is noted down by Carol-Erba 1106 C, H and N-analyzer.

For DSC, thermal experiments were recorded by a Perkin Elmer, DSC model, Jade DSC instrument at 10 $^{o}C\ min^{-1}$ in the presence of nitrogen.

Thermogravimetric thermograms were recorded using a Perkin Elmer. TGA mode, Pyris 1 at 10 ^{o}C min^{-1} in oxygen.

3.3 Method of Synthesis

Novel naphthalenetetracarboxylic diimide (TNDI) was successfully synthesized via condensation of 4,6-diamino-2- pyrimidinethiol with 1,4,5,8,-naphthalenetetracarboxylic dianhydride (NDA) using *m*-cresol/isoquinoline mixture as solvent.

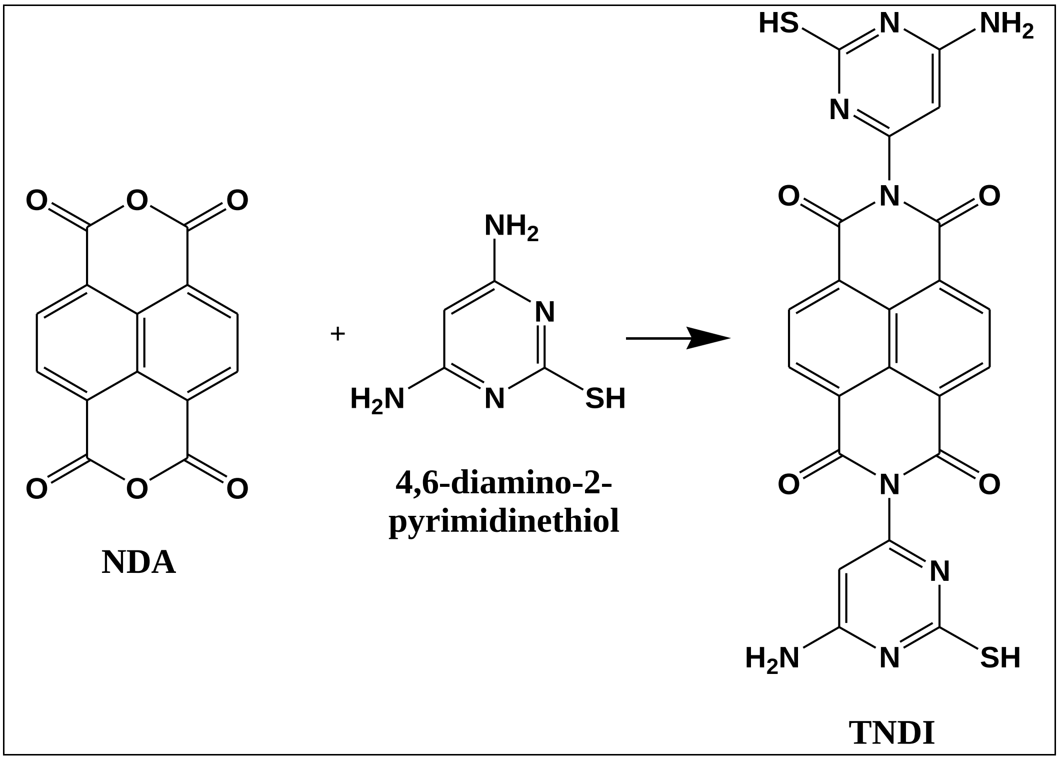

Scheme 1: Synthesis of TNDI

3.4 Synthesis of TNDI

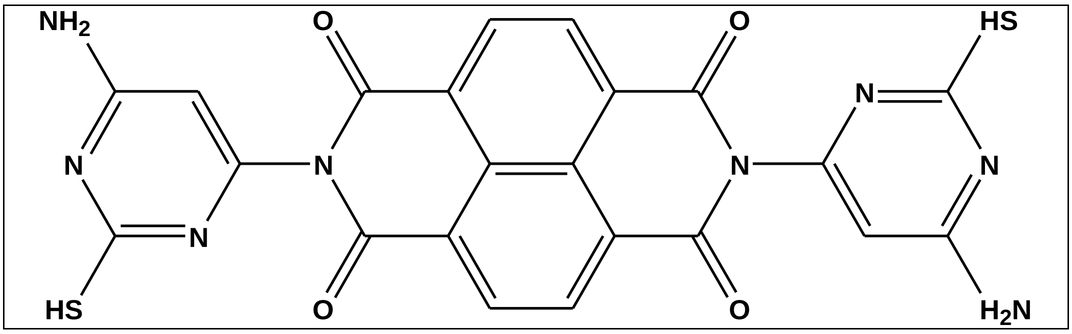

Scheme 2: Structure of TNDI

1,4,5,8,- naphthalenetetracarboxylic dianhydride (1.00 g, 3.73 mmol) and 4,6-Diamino-2-pyrimidinethiol (1.45g, 10.20 mmol) and $Zn(OAc)_2.2H_2O$ (0.997 g, 2.50 mmol) were heated with caution in the dried solvent mixture (40 mL *m*-cresol and 40 mL isoquinoline) under argon atmosphere at 100 °C for 2 h, 150 °C for 4 h, 170 °C for 2 h, 180 °C for 16 h and finally at 200 °C for 5 h. The solution was allowed to cool and then was poured into 300 mL of acetone. The precipitate was filtered off by suction filtration and subjected to dry at 100 °C under vacuum. The product was treated with acetone in a Soxhlet apparatus for 10 days (40 h) in order to get rid of unreacted amine, catalyst zinc acetate and high boiling point solvents. The purified compound was dried in vacuum oven at 100 °C after purification.

Yield: 65%

Color: Brown

FT-IR (KBr, cm^{-1}): 3437, 3392, 3190, 3130, 3070, 1720, 1682, 1630, 1577, 1442, 1382, 1337, 1255, 1202, 760

UV-vis (DMF) (λ_{max}, nm): 339, 357, 378

Fluorescence (DMF) (λ_{max}, nm): 434, 531

Anal. Calcd. for ($C_{22}H_{12}N_8O_4S_2$) (*M*$_w$, 516.51 g/mol), C, 51.16%; **H,** 2.34%; **N,** 21.69%; **S**, 12.42%; **O**, 12.39%

Found: C, 50.49%; **H**, 2.31%; **N**, 20.94%; **S**, 11.44%

3.5 General Synthesis Mechanisms of Naphthalene Dyes:

STEP 1

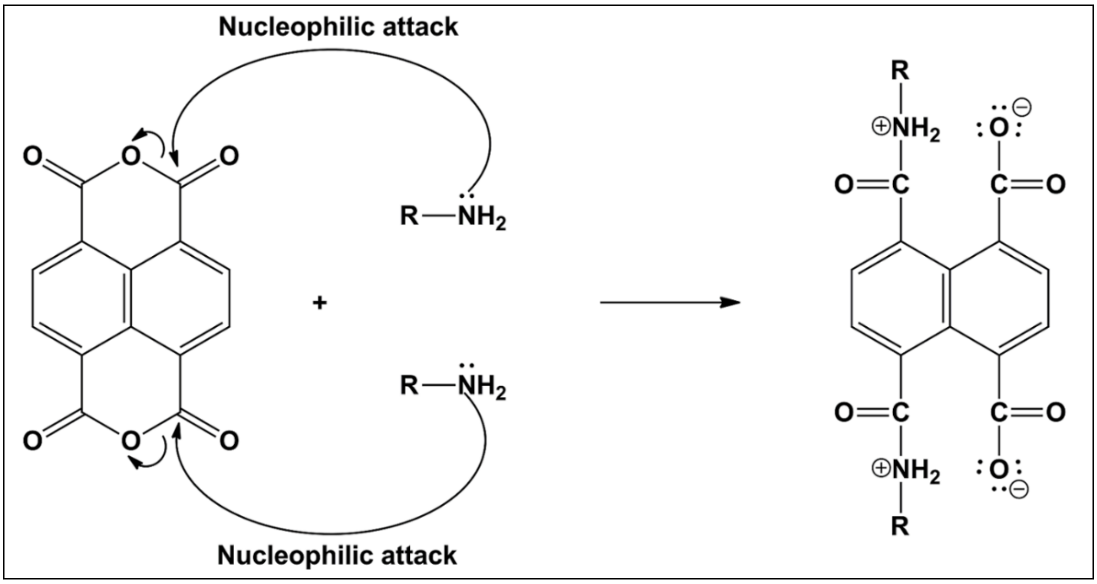

STEP 2

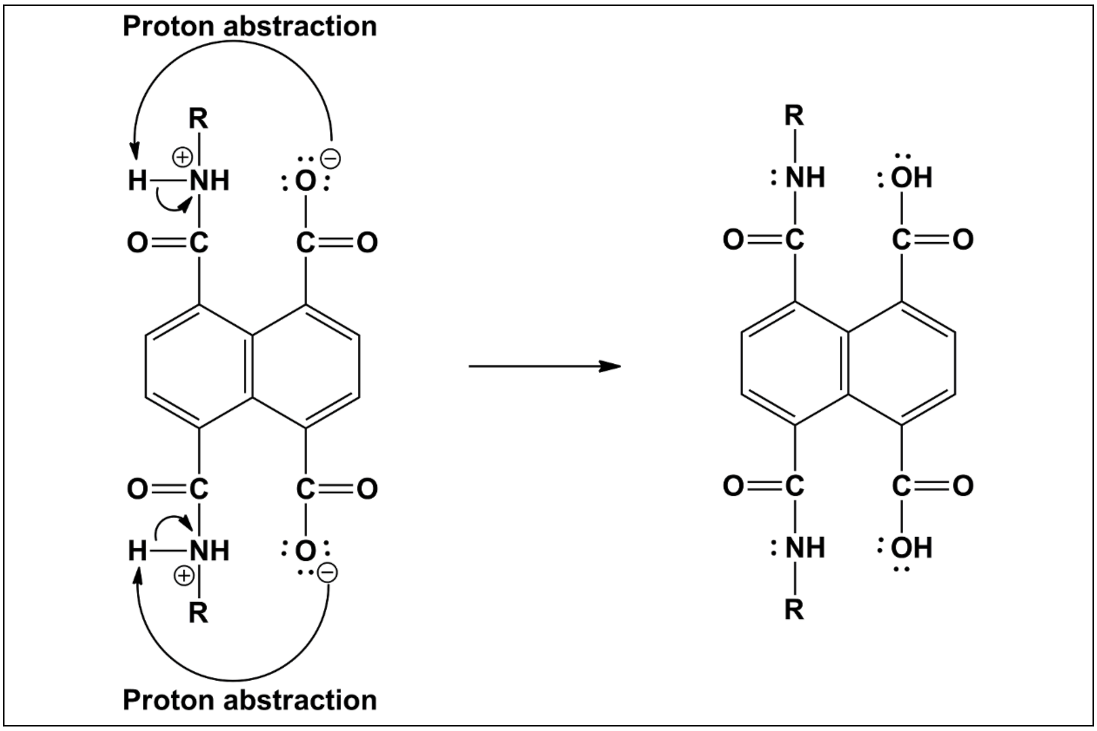

Proton abstraction
R
H
NH
O
C
Proton abstraction

STEP 3

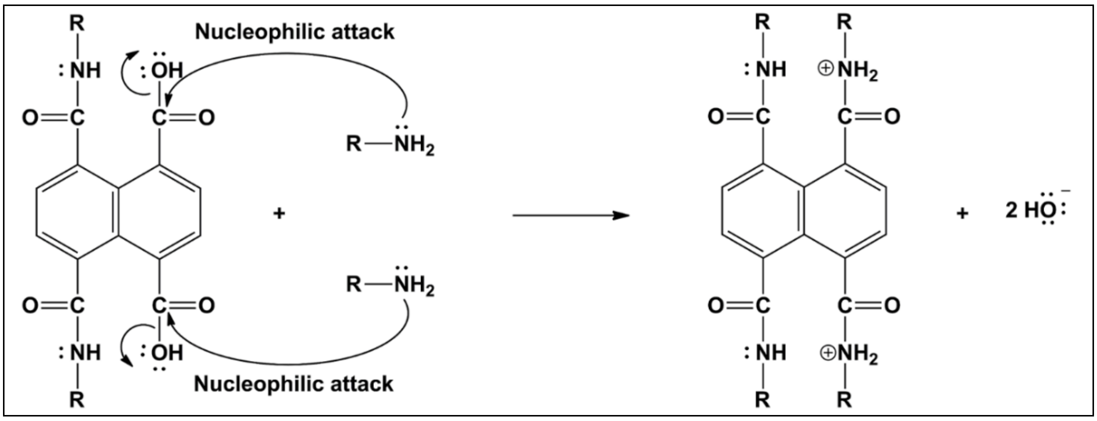

Nucleophilic attack
R—NH2
+
Nucleophilic attack
+
2 HO

STEP 4

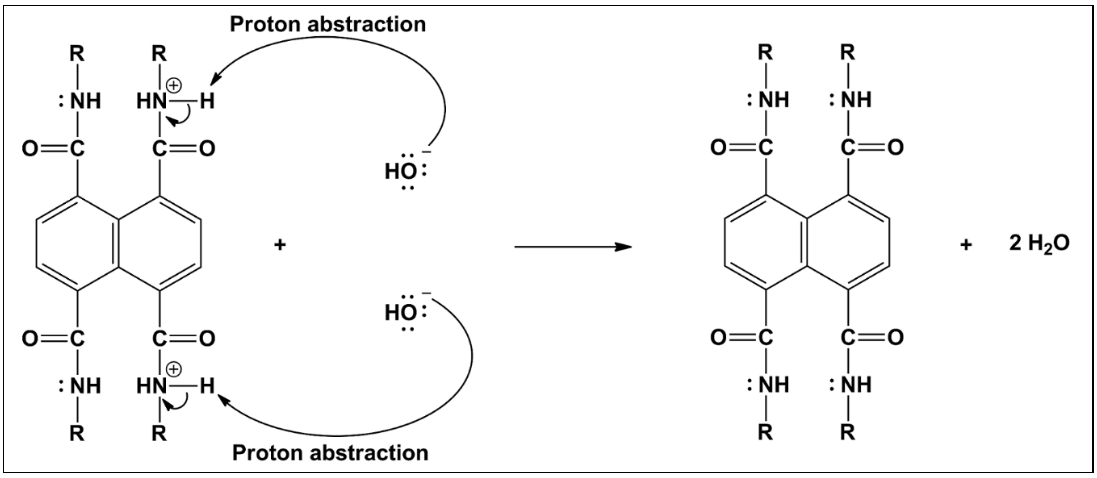

STEP5

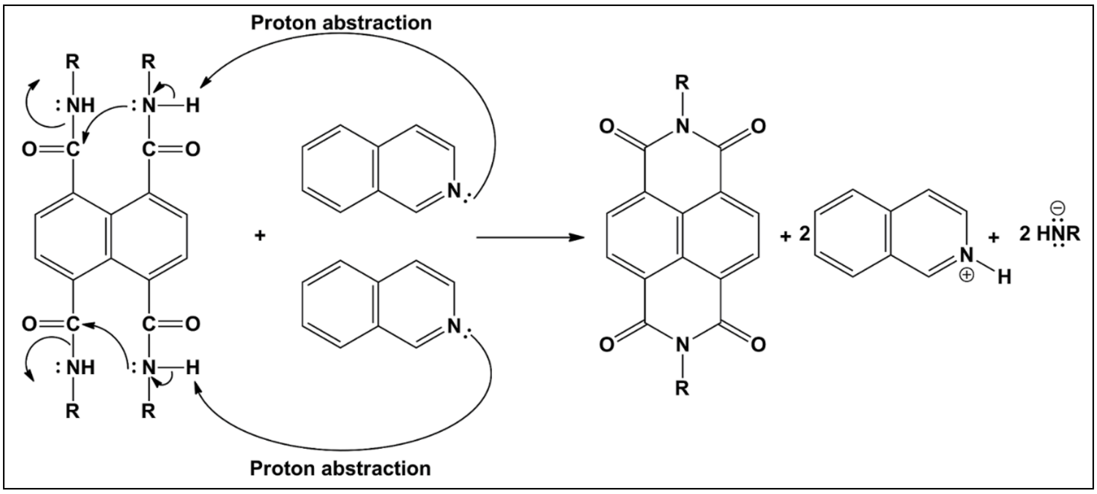

STEP 6

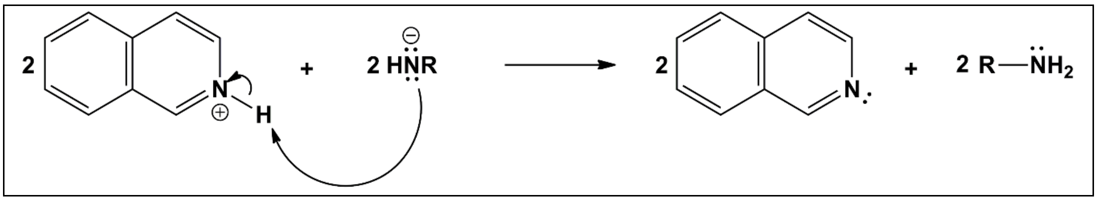

Chapter 4

DATA AND CALCULATION

4.1 Optical and Photochemical Properties

4.1.1 Molar Absorption Coefficient (ε_{max})

Beer Lambert's law (Eq. 4.1) is used to calculate molar absorbance coefficient. It is a measure of how strong chemical specie absorbs light at a particular wavelength per molar concentration.

$$\varepsilon_{max} = \frac{\mathrm{A}}{C \times l} \qquad \text{(Eq. 4.1)}$$

Where,

ε_{max} = molar extinction coefficient (L mol^{-1} cm^{-1})

A = Absorption of analyte at a wavelength

c = concentration of solution (mol L^{-1})

l = pathlength (cm)

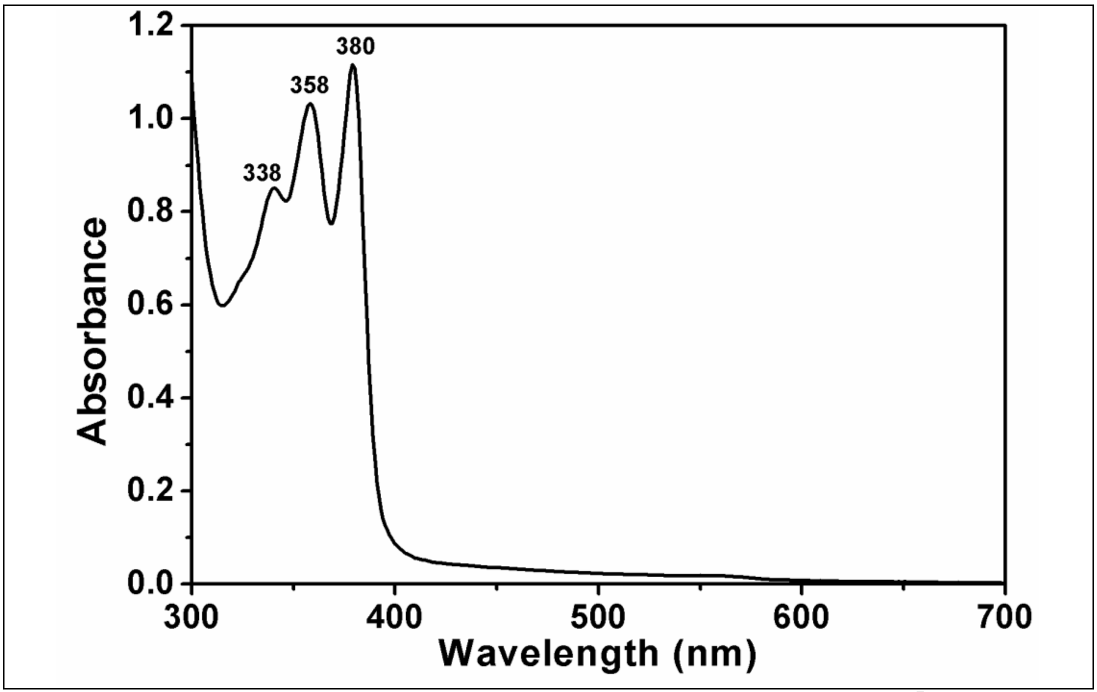

Figure 4.1: Absorbance Spectrum of TNDI in TFA at 1 × 10^{-5} M

ε_{max} of TNDI in TFA = 110000 (L. $Mol^{-1}.cm^{-1}$)

Table 4.1: Molar Absorptivity Data for TNDI in TFA, DMF and NMP

Solvents	Concentration (M)	Absorbance	λ_{max}	$\varepsilon_{max}(Lmol^{-1}cm^{-1})$
TFA	1×10^{-5}	1.1	380	110000
DMF	1×10^{-5}	0.7	379	70000
NMP	1×10^{-5}	0.727	360	72700

4.1.2 Florescence Quantum Yield (Φ_f)

The ratio of photons absorbed to the photons emitted is known as florescence quantum yield (Φ_f). Fluorescence quantum yield is calculated by using Eq. 4.2.

$$\Phi_f = \frac{A_{std}}{A_u} \times \frac{S_u}{S_{std}} \times (\frac{n_u}{n_{std}})^2 \times \Phi_{std} \qquad \text{(Eq. 4.2)}$$

Where,

Φ_f : Fluorescence quantum yield of unknown

A_{std}: Absorbance of the reference at the excitation wavelength

A_u : Absorbance of the unknown at the excitation wavelength

S_{std}: The integrated emission area across the band of reference

S_u : The integrated emission area across the band of unknown

n_{std}: Refractive index of reference solvent

n_u : Refractive index of unknown solvent

Φ_{std}: Fluorescence quantum yield of reference.

In the calculation of fluorescence quantum yield of TNDI anthracene was used as reference. The fluorescence quantum yield of anthracene is 0.27 in ethanol (Aleshinloye A. O, Icil H 2015).

The excitation wavelength of TNDI and reference are 360 nm.

The fluorescence quantum yield of TNDI in NMP:

Φ_f(std)= 0.27 in EtOH

A_{std}= 0.1055

A_u= 0.119

S_{std}= 7827.32

$S_u = 2725$

n_{std}= 1.361

n_u= 1.47

$$\Phi_f = \frac{0.1055}{0.119} \times \frac{2725}{7827.32} \times \left(\frac{1.47}{1.361}\right)^2 \times 0.27 = 0.09$$

Table 4.2: Fluorescence quantum yields of TNDI in DMF and NMP solvents

Solvents	**Φ_f**
DMF	0.075
NMP	0.09

4.1.3 Half width of the designated absorption band ($\Delta\bar{\upsilon}_{1/2}$)

Equantion 4.3 is used to calculate half-width of maximum absorption band.

$\Delta\bar{\upsilon}_{1/2} = \bar{\upsilon}_1 - \bar{\upsilon}_2$ (Eq. 4.3)

Where,

$\Delta\bar{\upsilon}_{1/2}$ = Half width of the designated absorption maximum (cm^{-1})

$\bar{\upsilon}_1 - \bar{\upsilon}_2$ = the estimated frequencies from the absorption of compound

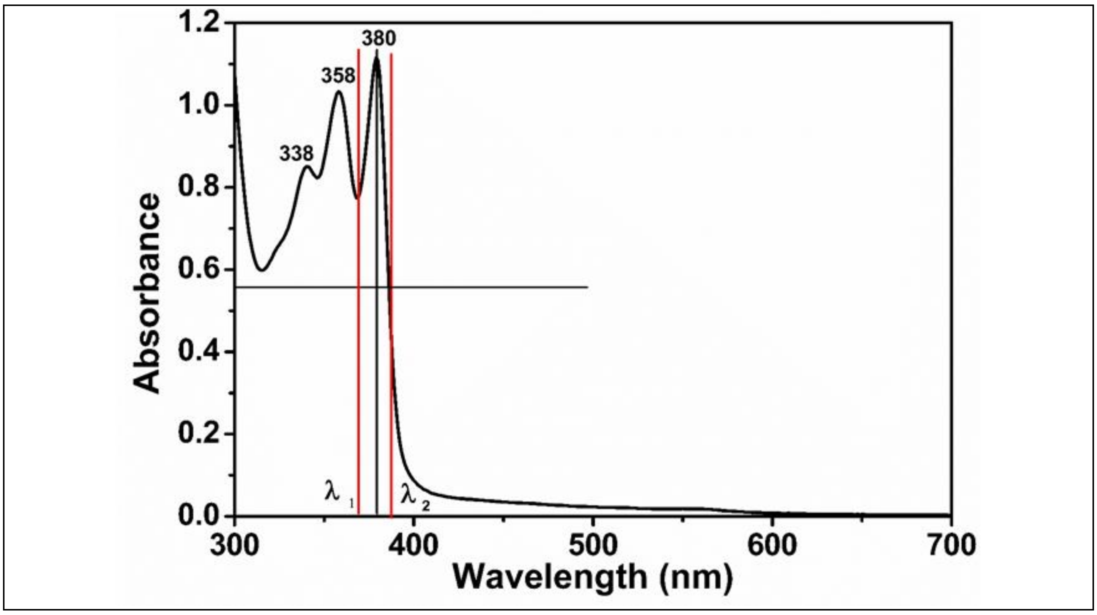

Figure 4.2: Representative Half-Width plot on the Absorption spectrum of TNDI in TFA

From figure 4.2 λ_1= 375 nm

$$375 \text{ nm} \times \frac{10^{-9}m}{1nm} \times \frac{1cm}{10^{-2}m} = 3.75 \times 10^{-5} \text{ cm}$$

$$\bar{\upsilon}_1 = \frac{1}{\lambda_1} = \frac{1}{3.75 \times 10^{-5}cm} = 26666{\cdot}67 \text{ cm}$$

λ_2 = 384 nm

$$384 \text{ nm} \times \frac{10^{-9}}{1nm} \times \frac{1cm}{10^{-2}} = 3.84 \times 10^{-5} cm^{-1}$$

$$\bar{\upsilon}_2 = \frac{1}{\lambda_2} = \frac{1}{3.84 \times 10^{-5}} = 26041.67\ cm^{-1}$$

$$\Delta\bar{\upsilon}_{1/2} = \bar{\upsilon}_1 - \bar{\upsilon}_2 = 625\ cm^{-1}$$

Correspondingly, for dissimilar solvents the half-width were determined as given in Table 4.3.

Table 4.3: Half-width of TNDI in different solvents

Solvent	**λ_1**	**λ_2 (nm)**	**$\bar{\upsilon}_1$**	**$\bar{\upsilon}_2$ (cm^{-1})**	**$\Delta\bar{\upsilon}_{1/2}$ (cm^{-1})**
TFA	375	384	26666.67	26041.67	625
DMF	265	279	37735.85	35842.29	1893.55
NMP	353	365	28169.01	27397.26	771.75

4.1.4 Theoretical Radiative Lifetime (τ_0)

Theoretical radiative lifetime is calculated by using Equation 4.4.

$$\tau_0 = \frac{3.5 \times 10^8}{\bar{\upsilon}_{max}{}^2 \times \varepsilon_{max} \times \Delta\bar{\upsilon}_{1/2}} \qquad \text{(Eq. 4.4)}$$

Where τ_0 = theoretical radiative lifetime (ns)

$\bar{\upsilon}_{max}$ = mean frequency of the maximum absorption band (cm^{-1})

ε_{max} = maximum absorption coefficient ($Lmol^{-1}cm^{-1}$)

$\Delta\bar{\upsilon}_{1/2}$ = Half width of the designated absorption maximum (cm^{-1})

The Theoretical Radiative Lifetime of TNDI in TFA is calculated as follows using values of molar absorptivity and half-width of designated absorption:

From figure 4.1 and 4.2 λ_{max}=380 nm

$380 \text{ nm} \times \frac{10^{-9}m}{1nm} \times \frac{100cm}{1m} = 3.8 \times 10^{-5}$

$\bar{\upsilon}_{max} = \frac{1}{\lambda_{max}} = \frac{1}{3.8\times10^{-5}cm} = 26315.79\ cm^{-1}$

$\Delta\bar{\upsilon}^2_{max} = (26315.79\ cm^{-1})^2 = 6.925\times 10^8 cm^{-2}$

$\Delta\bar{\upsilon}_{1/2} = 625\ cm^{-1}$

$$\tau_0 = \frac{3.5\times10^8}{6.925\times10^8\times110000\times625} = 7.351 \times 10^{-9}s$$

$$\tau_0 = 7.351 \times 10^{-9}s \times \frac{1_{ns}}{10_s^{-9}} = 7.351 \text{ ns}$$

Table 4.4: Theoretical Radiative Lifetime of TNDI in different solvents

solvents	**λ_{max}(nm)**	ε**max**(**LM** $^{-1}$**cm** $^{-1}$)	$\bar{\upsilon}^2_{max}$(**cm** $^{-1}$) ^{2}	$\Delta\bar{\upsilon}_{1/2}(cm^{-1})$	**τ_0(ns)**
TFA	380	110000	6.925×10^8	625	7.351
DMF	379	70000	6.961×10^8	1893.55	3.793
NMP	360	72700	7.716×10^8	771.75	8.084

4.1.5 Theoretical Fluorescence Life Time (τ_f)

The theoretical fluorescence lifetime refers to the theoretical average time of the molecule stays in the excited state before florescence (emitting photon).

For calculation of theoretical fluorescence lifetime Eq. 4.5 is used [Turro's Equation].

$$\tau_f = \tau_0 \times \Phi_f \qquad \text{(Eq. 4.5)}$$

Theoretical Fluorescence Life Time of TNDI in NMP

$\tau_f = 7.351 \times 0.09 = 0.66$ ns

The table 4.5 represents the calculated theoretical fluorescence lifetime of TNDI in NMP and DMF as solvents.

Table 4.5: Theoretical fluorescence lifetime in different solvents

Solvents	**$\tau_{0(ns)}$**	**Φ_f**	**τ_f**
DMF	3.793	0.075	0.28
NMP	8.084	0.09	0.66

4.1.6 Fluorescence Rate Constants (k_f)

Fluorescence rate constant is calculated by using Equation 4.6.

$$K_f = \frac{1}{\tau_0} \qquad \text{(Eq. 4.6)}$$

Where,

K_f= fluorescence rate constant (s^{-1})

And τ_0 = theoretical radiative lifetime (s)

K_f calculation of TNDI in TFA:

$$K_f = \frac{\mathbf{1}}{\mathbf{7.351 \times 10^{-9}\ s}} = 1.36 \times 10^8\ s^{-1}$$

Table 4.6: Theoretical fluorescence lifetime of TNDI in different solvents

solvents	$\boldsymbol{\tau_0}$	$\boldsymbol{K_f}$ ($\boldsymbol{s^{-1}}$)
TFA	7.351	1.36×10^{8}
DMF	3.793	2.63×10^{8}
NMP	8.084	1.23×10^{8}

4.1.7 Rate Constants of Radiation less Deactivation (k_d)

The k_d values of TNDI was determined using Eq. 4.7 as shown below.

$$K_d = (\frac{K_f}{\Phi_f}) - K_f \qquad \text{(Eq. 4.7)}$$

K_d calculation of TNDI in NMP

$$K_d = \left(\frac{1.23 \times 10^8 s^{-1}}{0.09}\right) - 1.23 \times 10^8 s^{-1} = 1.24 \times 10^9\ s^{-1}$$

Table 4.7: Radiation less deactivation rate constant of TNDI

Solvents	K_f	Φ_f	K_d **(**s^{-1}**)**
DMF	2.63×10^8	0.075	3.24×10^9
NMP	1.23×10^8	0.09	1.24×10^9

4.1.8 Oscillator Strengths (*f*)

The expression of the electronic transition strength is illustrated in terms of the dimensionless quantity of oscillator strength. Oscillator strength was determined using Eq. 4.8[Turro's Equation].

$$f = 4.32 \times 10^{-9} \times \Delta\bar{\upsilon}1/2 \times \varepsilon_{max} \quad \text{(Eq. 4.8)}$$

Where,

f = oscillator strength

$\Delta\bar{\upsilon}_{1/2}$ = half width of the designated absorption (cm^{-1})

ε_{max} = maximum absorption coefficient (L$mol^{-1}cm^{-1}$)

Oscillator Strengths of TNDI in NMP

$f = 4.32 \times 10^{-9} \times 771.75 \times 72700 = 0.242$

Oscillator Strengths of TNDI was calculated in various solvents and Table 4.8 Provides the Oscillator Strengths.

Table 4.8: Oscillator Strength data of TNDI in various solvent.

Solvents	ε_{max} **($M^{-1}.cm^{-1}$)**	$\Delta\bar{\upsilon}_{1/2}$ **(cm^{-1})**	***f***
TFA	110000	625	0.297
DMF	70000	1893.55	0.573
NMP	72700	771.75	0.242

4.1.9 Singlet Energies (E_s)

Singlet energy is the minimum amount of energy required for a chromophore/fluorophore to get excited from ground state to an excited state. Turro's equation (Eq. 4.9) was used to calculate the singlet energy.

$$E_s = \frac{2.86\times10^5}{\lambda_{max}} \qquad \text{(Eq. 4.9)}$$

Where,

E_s = singlet energy (kcal mol^{-1})

λ_{max} = maximum absorption wavelength ($\mathring{A}$)

E_s of TNDI in NMP

λ_{max} = 360 nm

$$E_s = 360 \times \frac{10\,\mathring{A}}{1_{nm}} = 3600\ \mathring{A}$$

$$E_s = \frac{2.85\times10^5}{3600} = 97.44 \text{ kcal mol}^{-1}$$

The singlet energies is calculated for TNDI in various solvents and listed in Table 4.9.

Table 4.9: singlet energy of TNDI in various solvents

Solvents	**λ_{max}(nm)**	**E_s(kcal mol^{-1})**
TFA	380	75.26
DMF	379	75.46
NMP	360	97.44

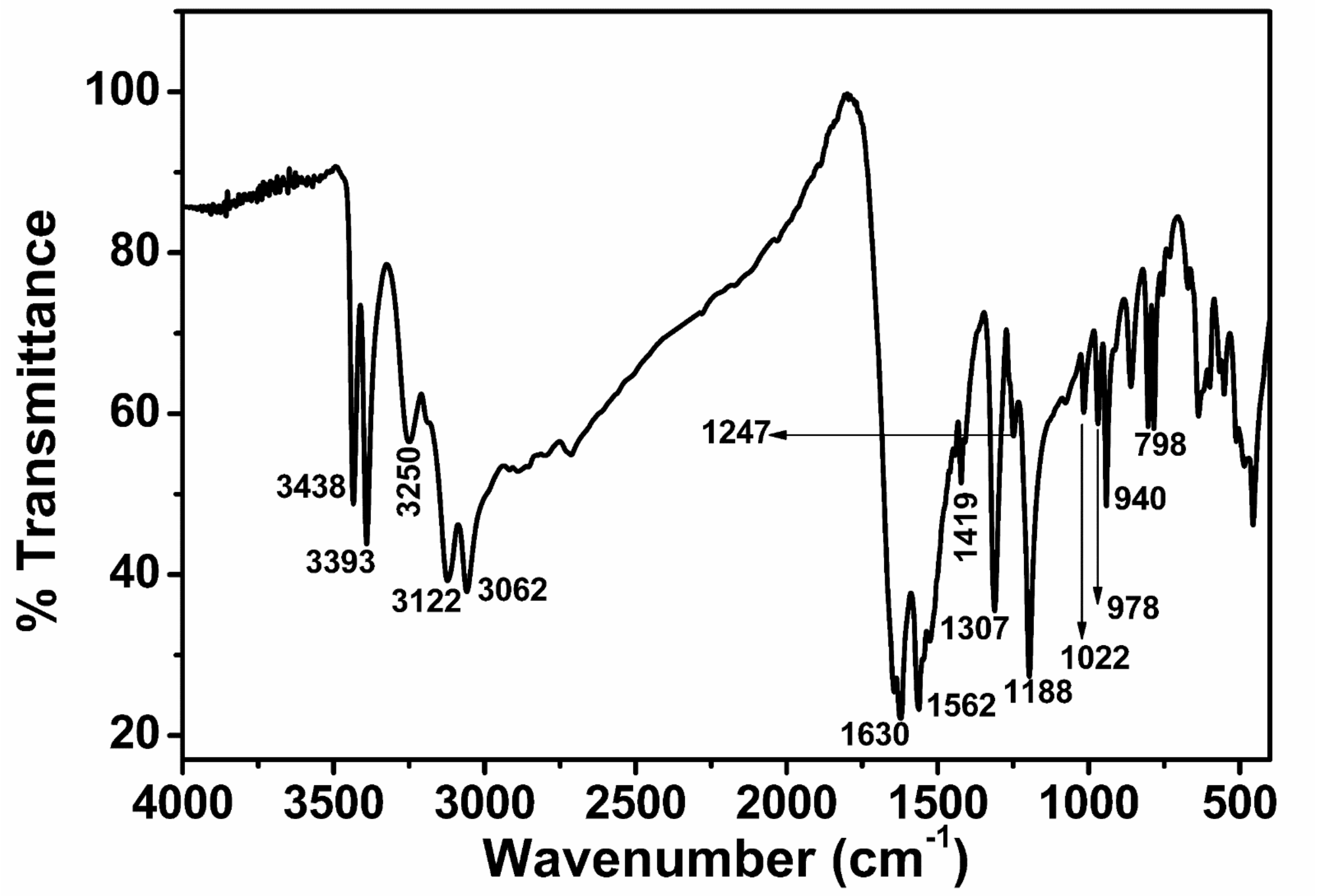

Figure 4.3: FTIR spectrum of 4, 6-Diamino-2-pyrimidin-thiol

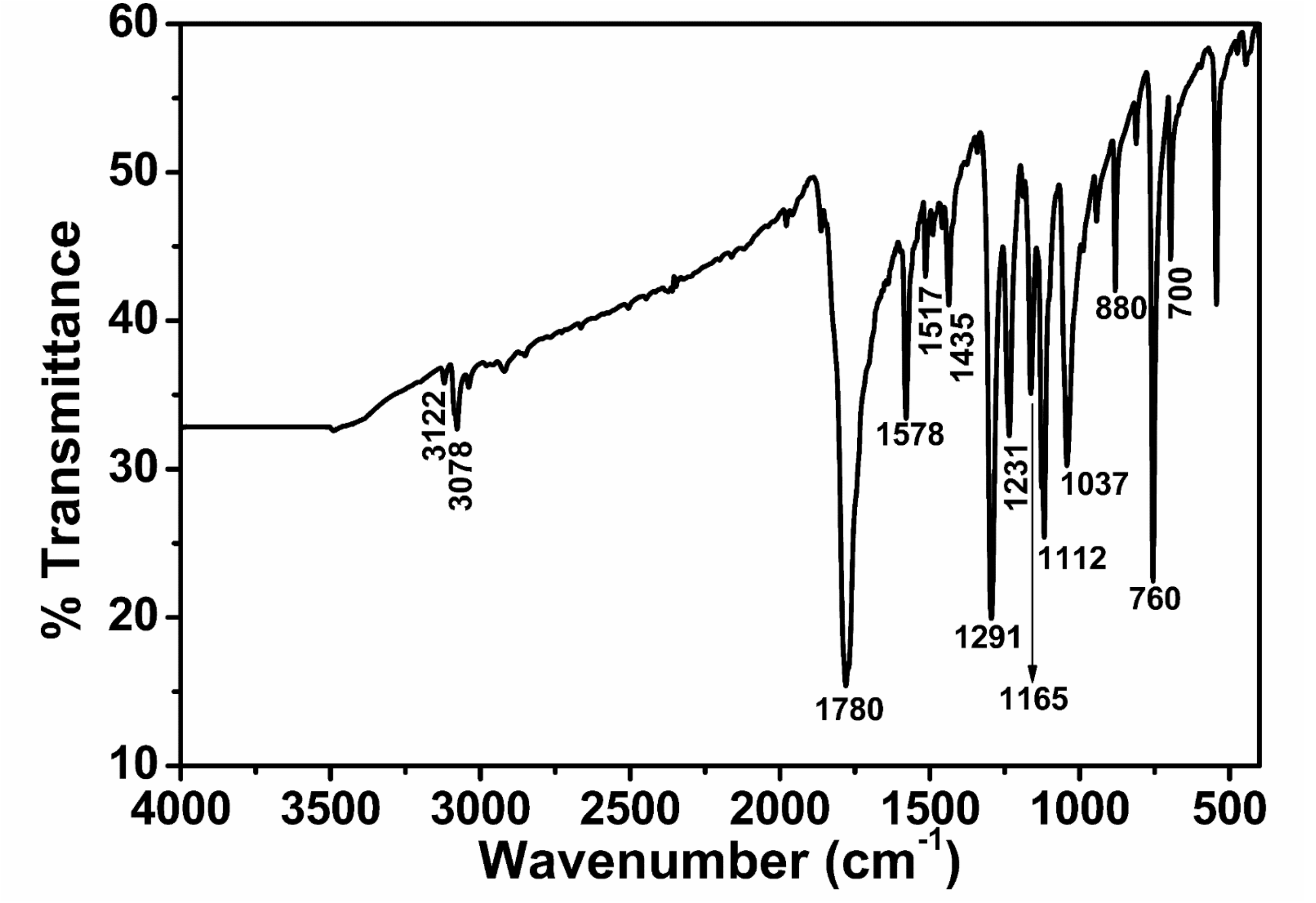

Figure 4.4: FTIR spectrum of Naphthalene anhydride

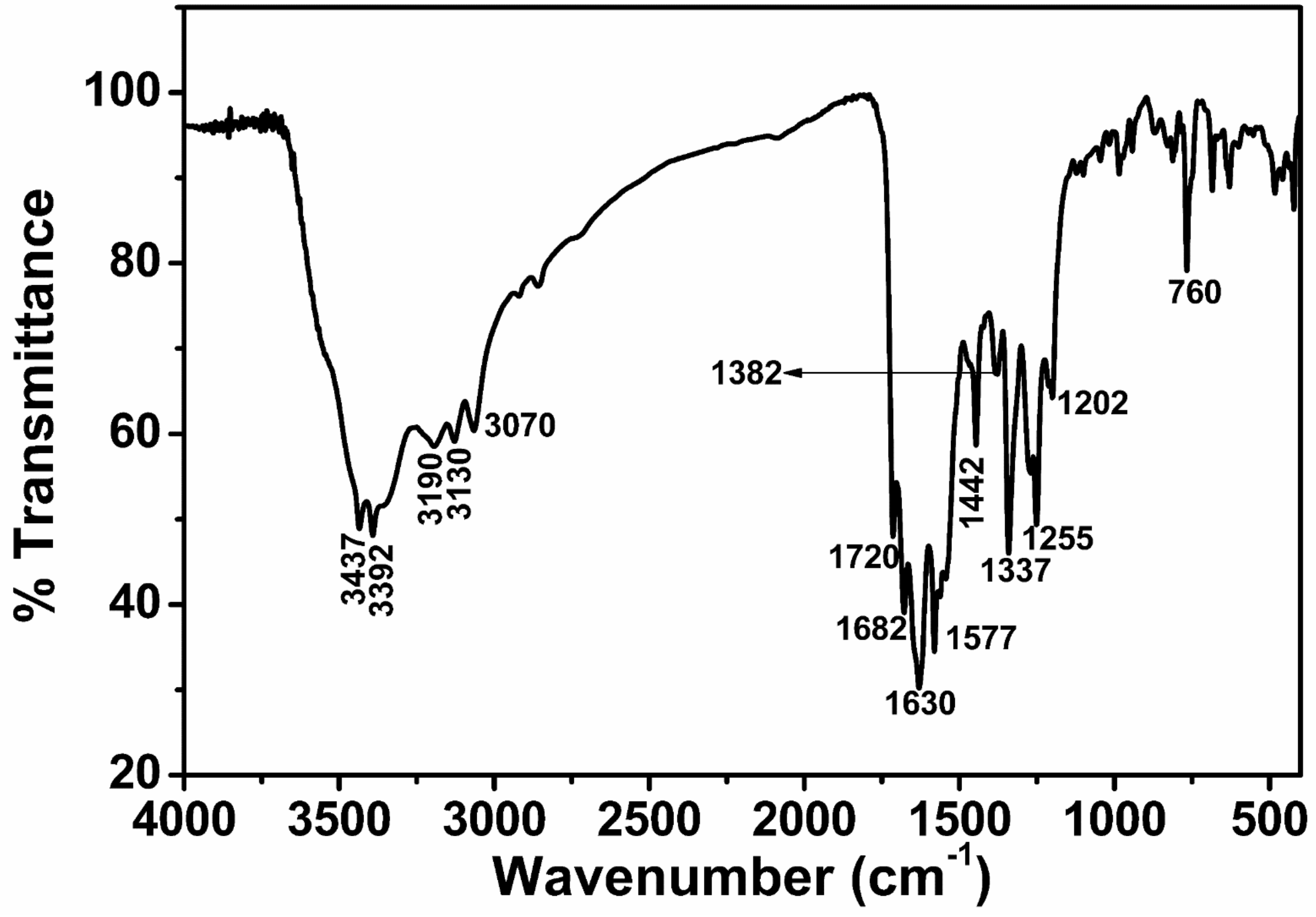

Figure 4.5: FTIR spectrum of TNDI

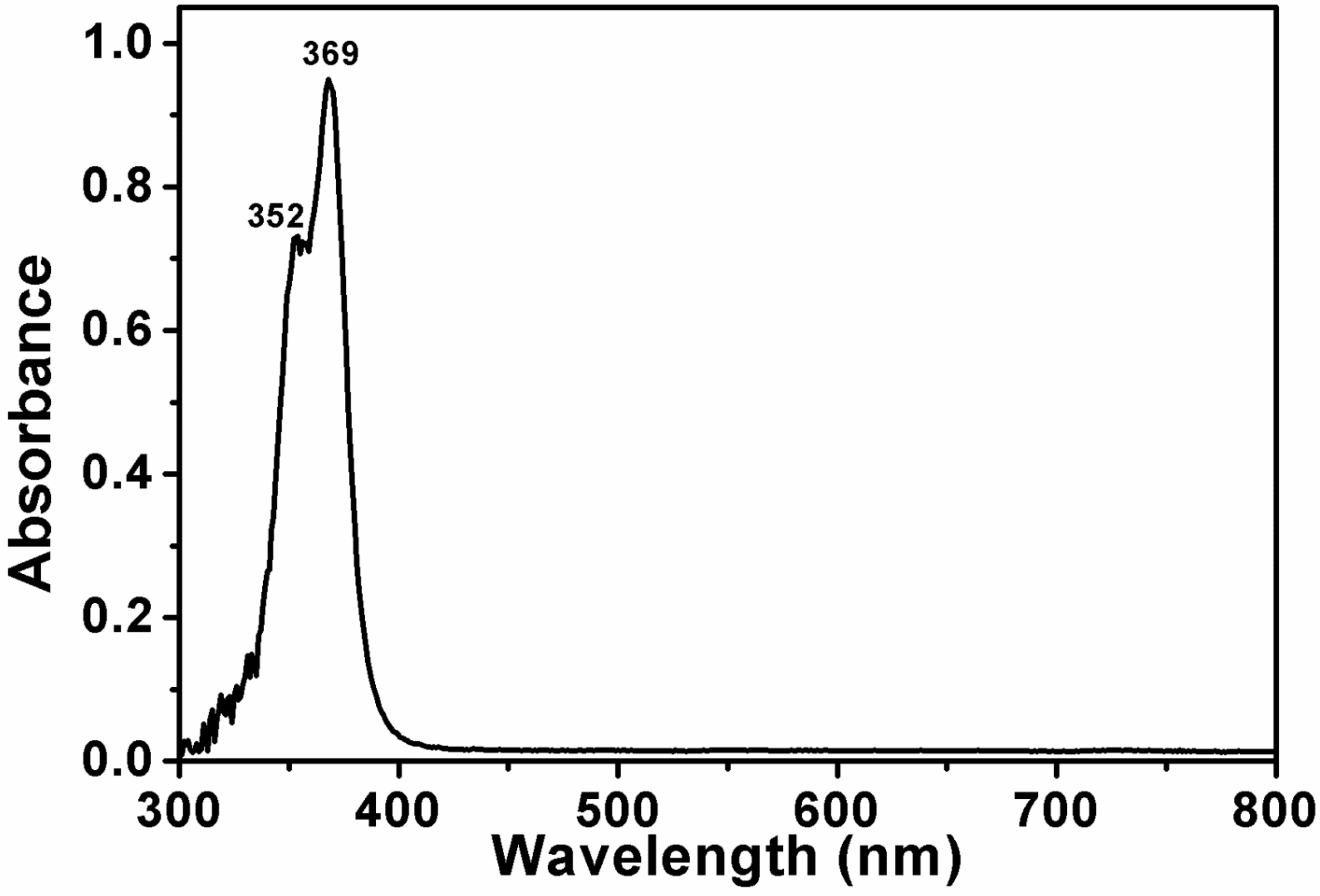

Figure 4.6: Absorption spectrum of 4, 6-Diamino-2-pyrimidin-thiol in DMF

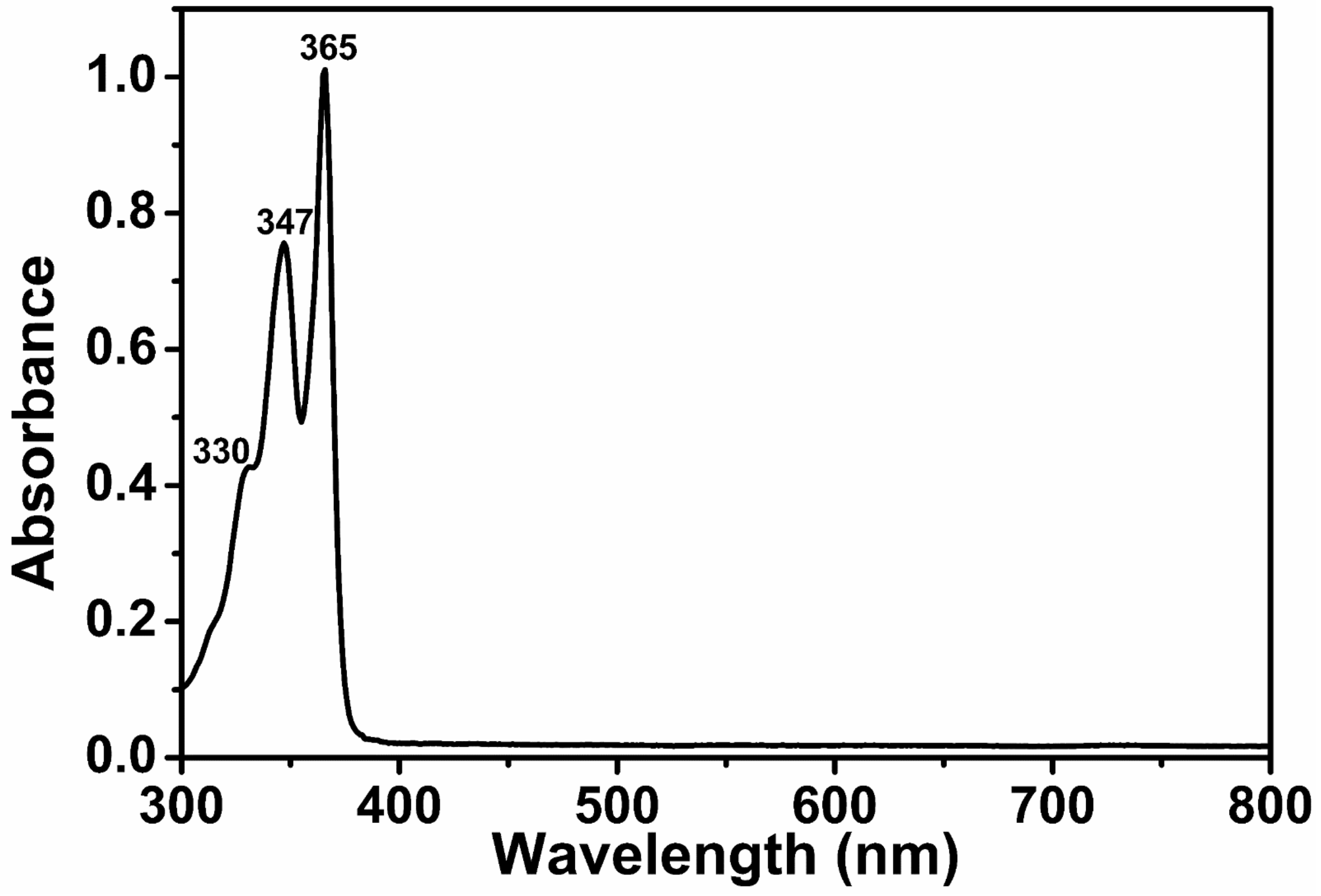

Figure 4.7: Absorption spectrum of Naphthalene anhydride in DMF

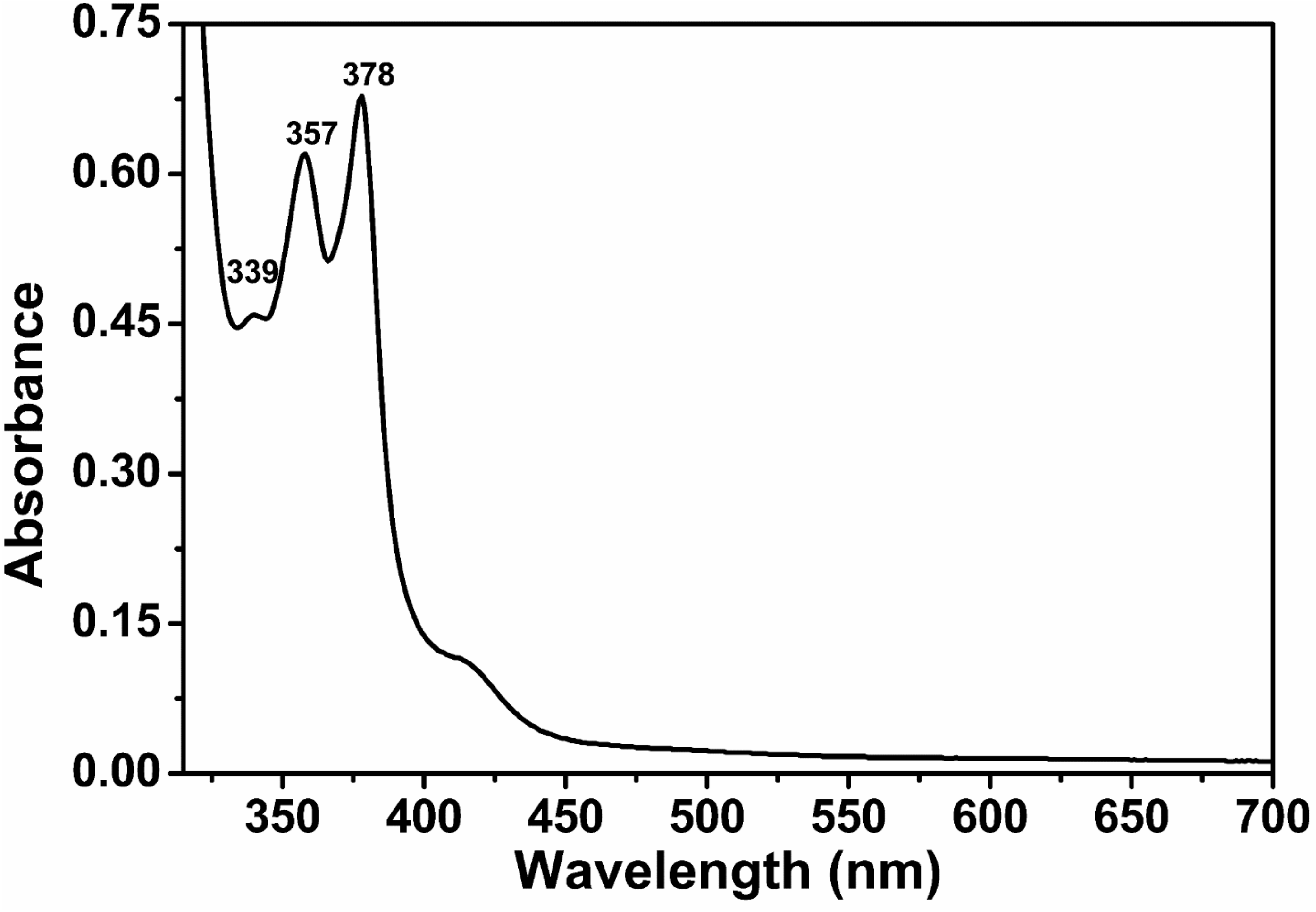

Figure 4.8: Absorption spectrum of TNDI in DMF

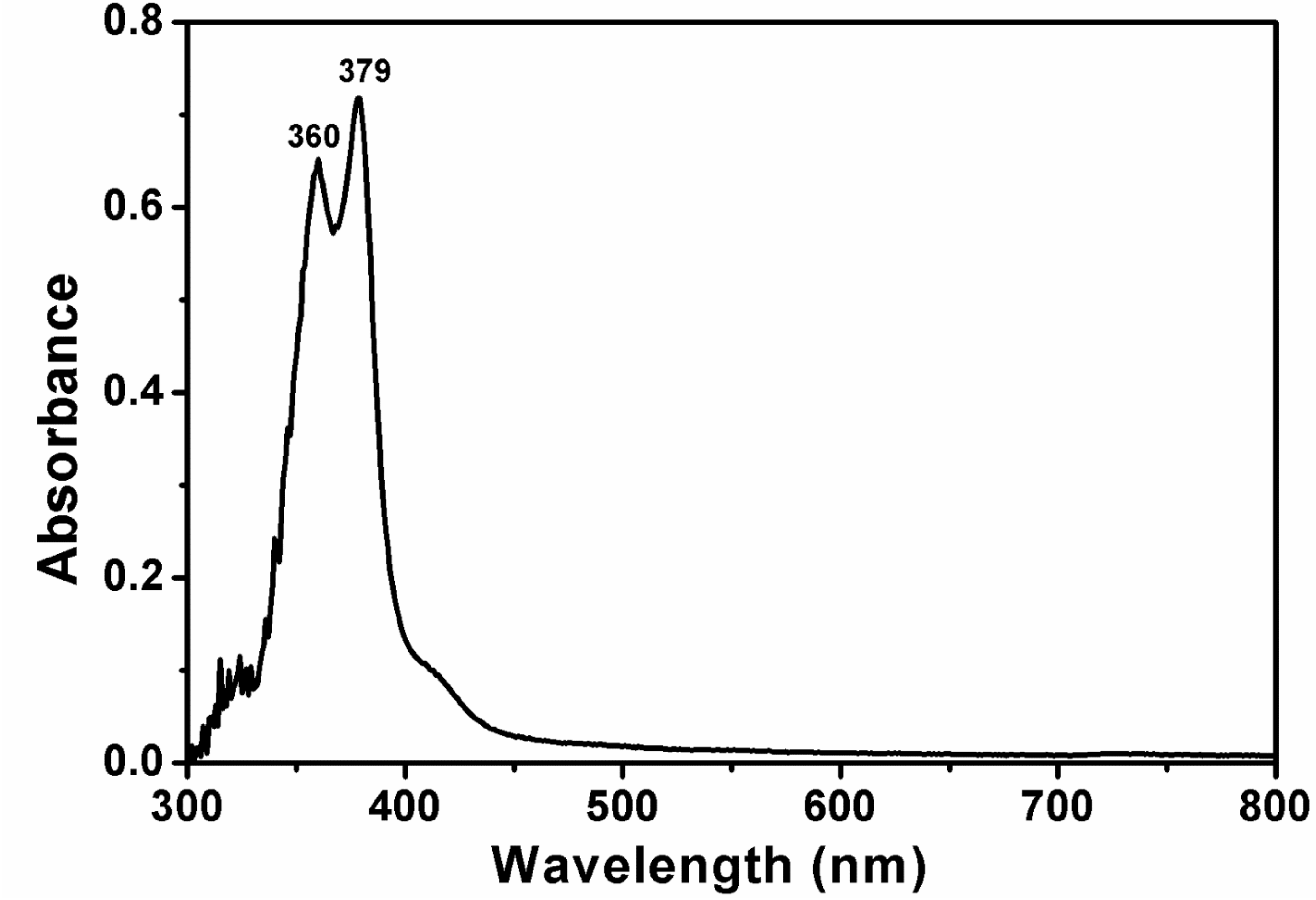

Figure 4.9: Absorption spectrum of TNDI in DMF after microfiltration (0.2µm)

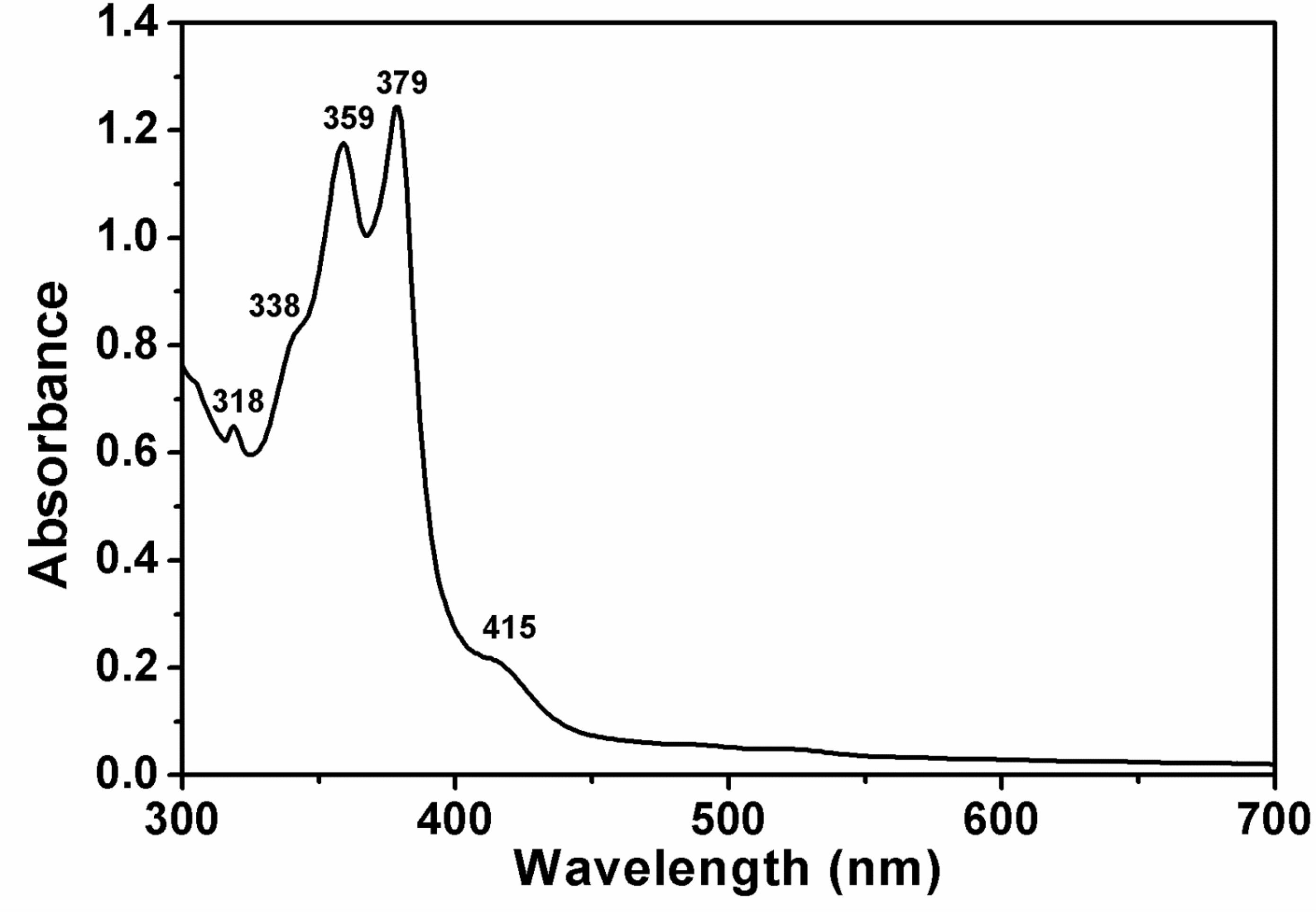

Figure 4.10: Absorption spectrum of TNDI in NMP

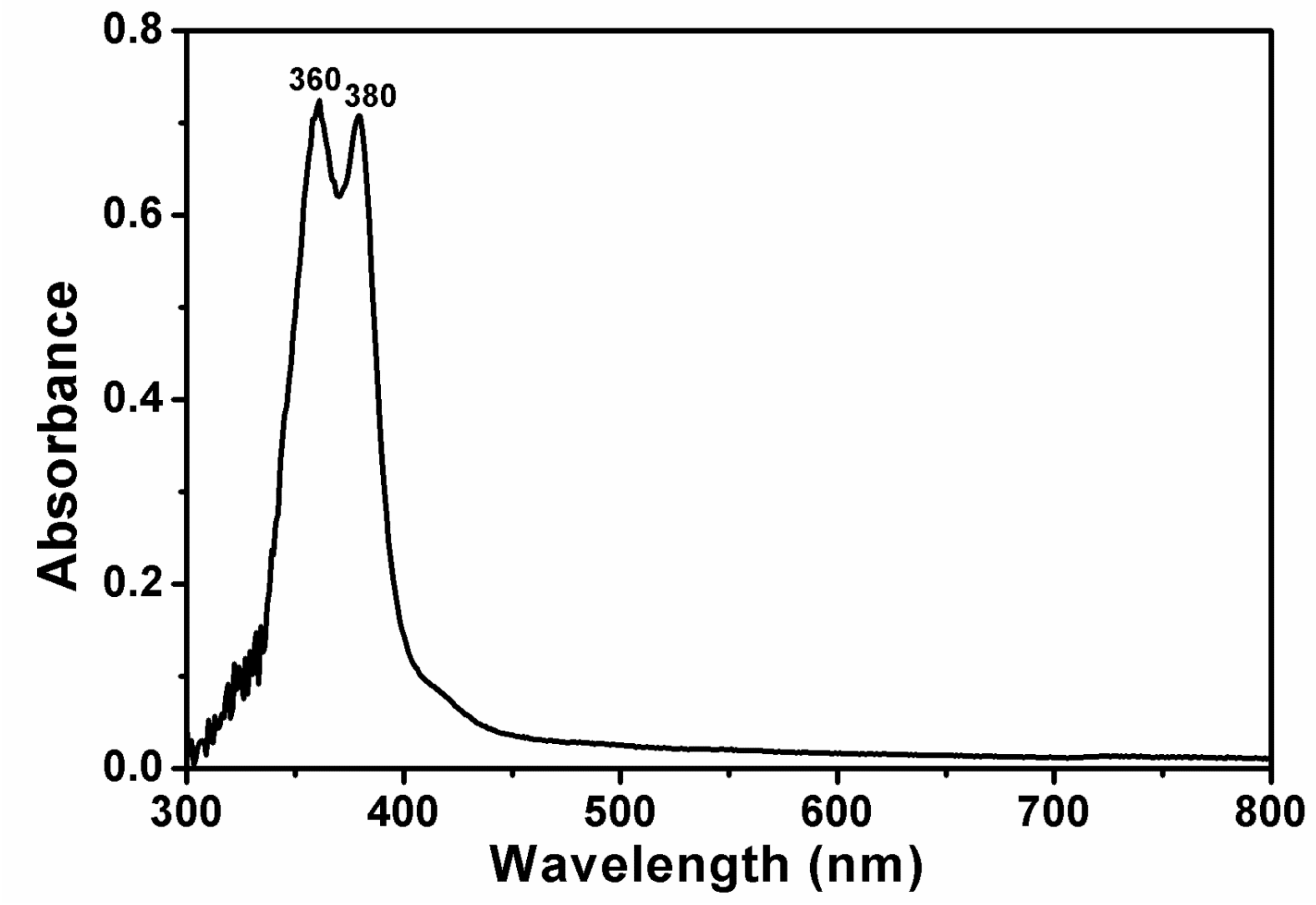

Figure 4.11: Absorption spectrum of TNDI in NMP after microfiltration (0.2µm)

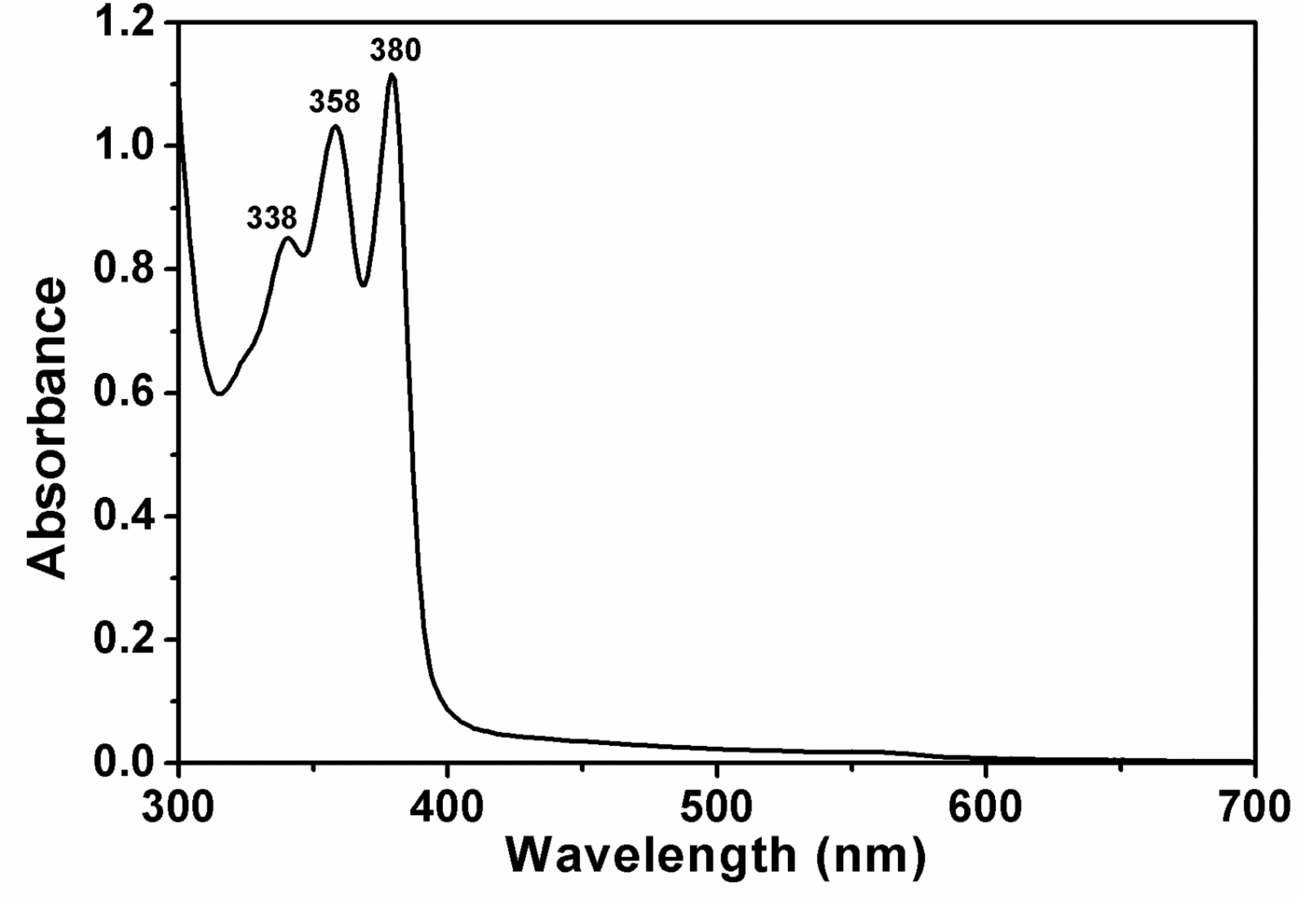

Figure 4.12: Absorption spectrum of TNDI in TFA

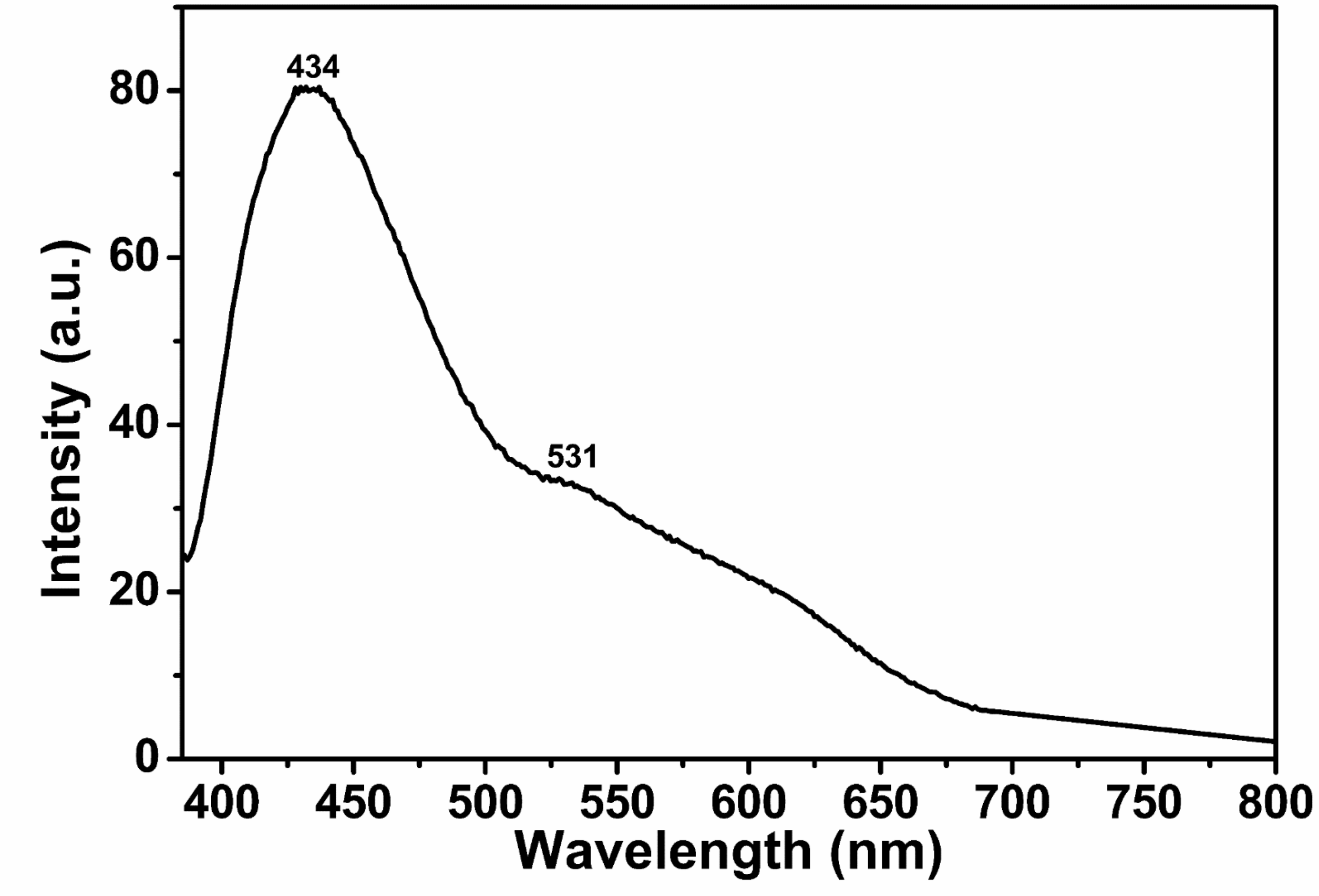

Figure 4.13: Emission spectrum of TNDI in DMF

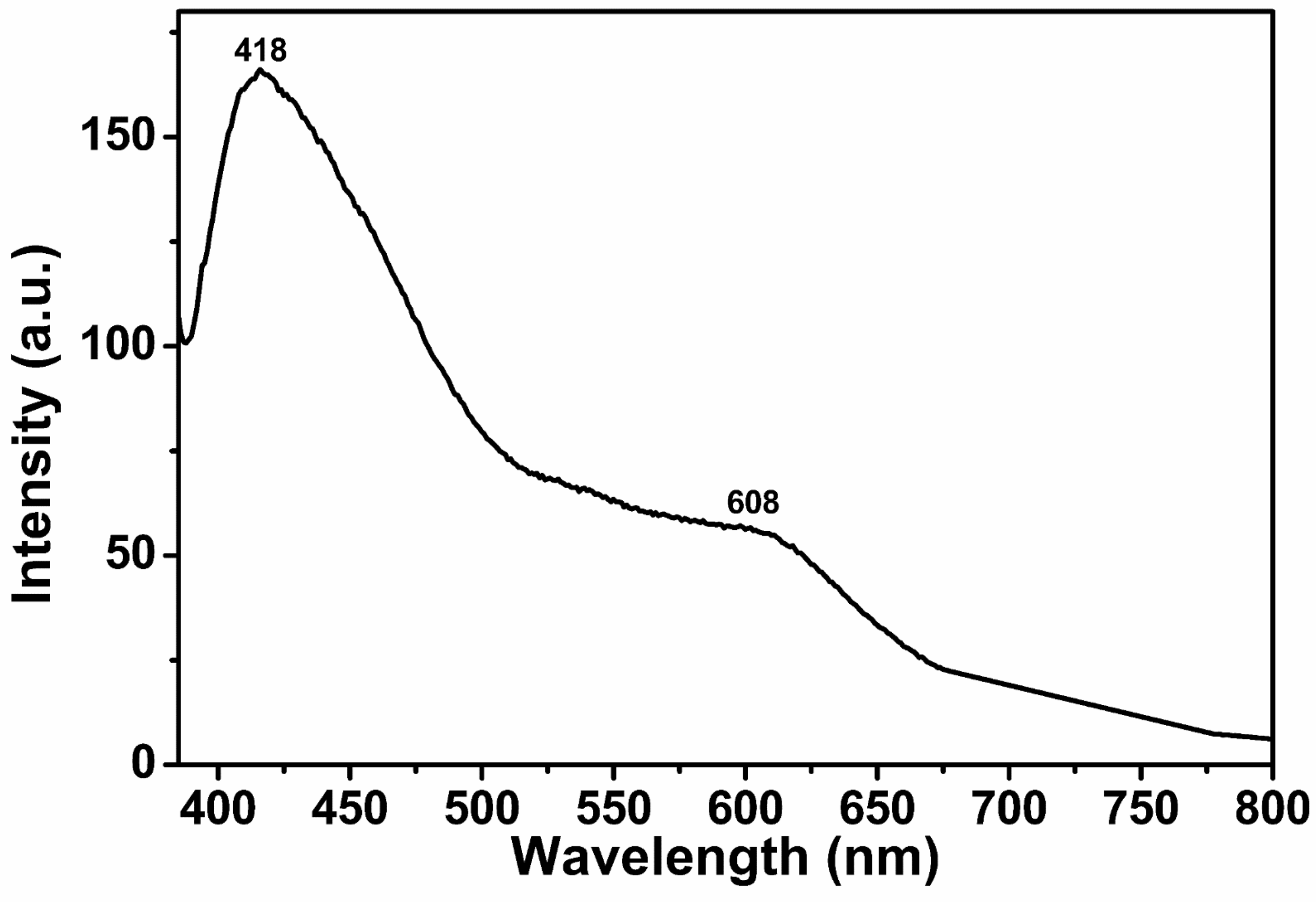

Figure 4.14: Emission spectrum of TNDI in DMF after microfiltration (0.2µm)

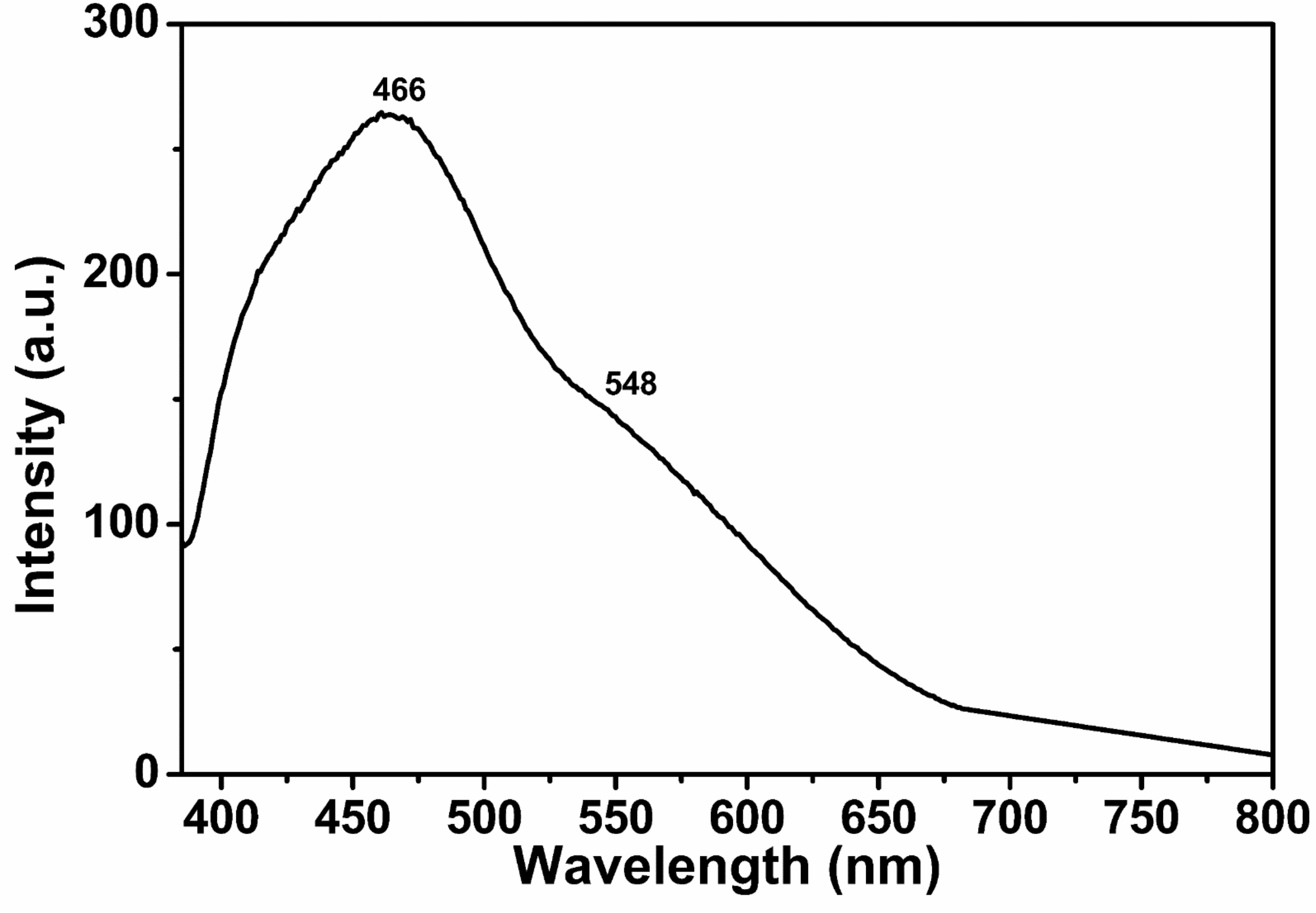

Figure 4.15: Emission spectrum of TNDI in NMP

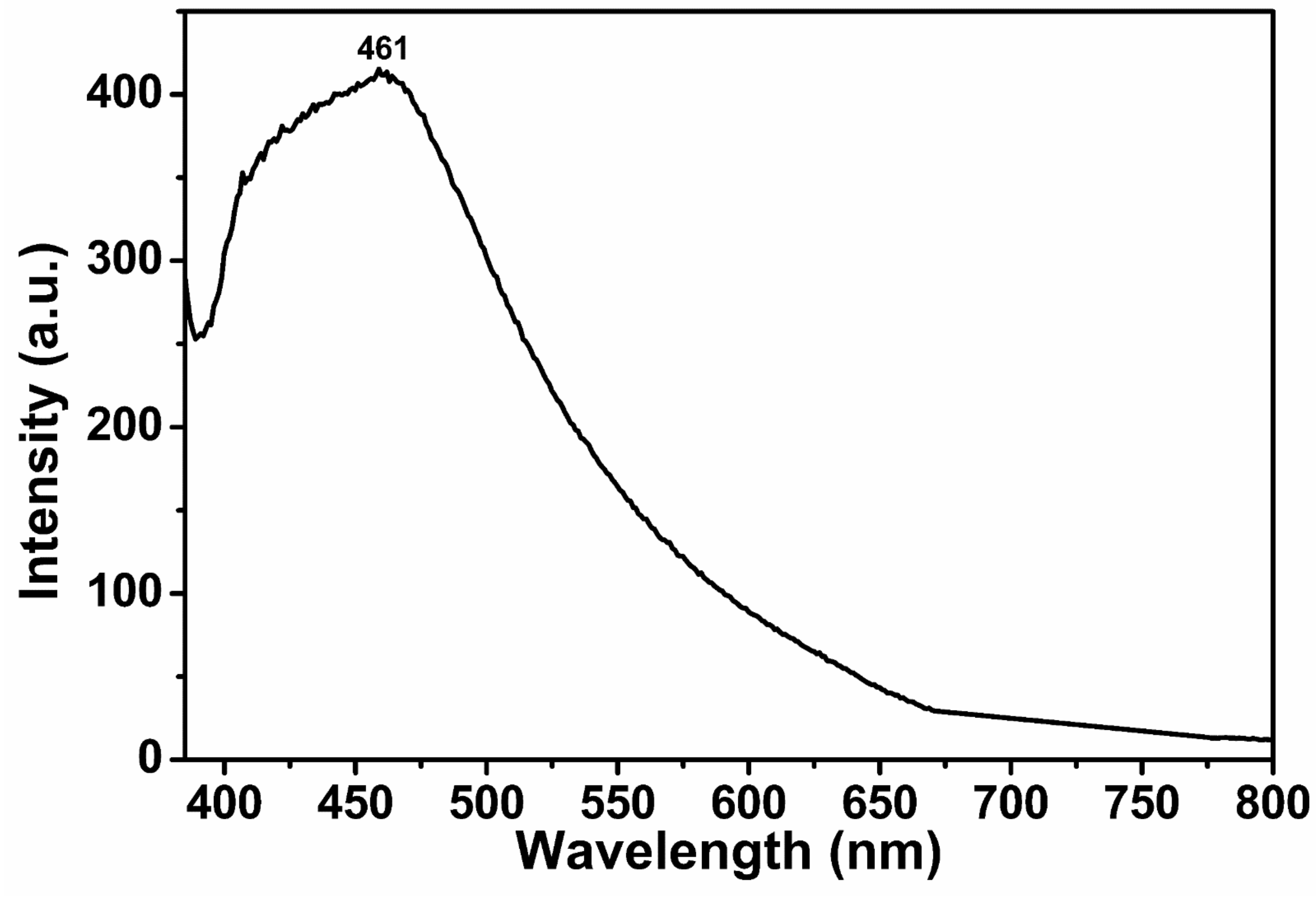

Figure 4.16: Emission spectrum of TNDI in NMP after microfiltration (0.2µm)

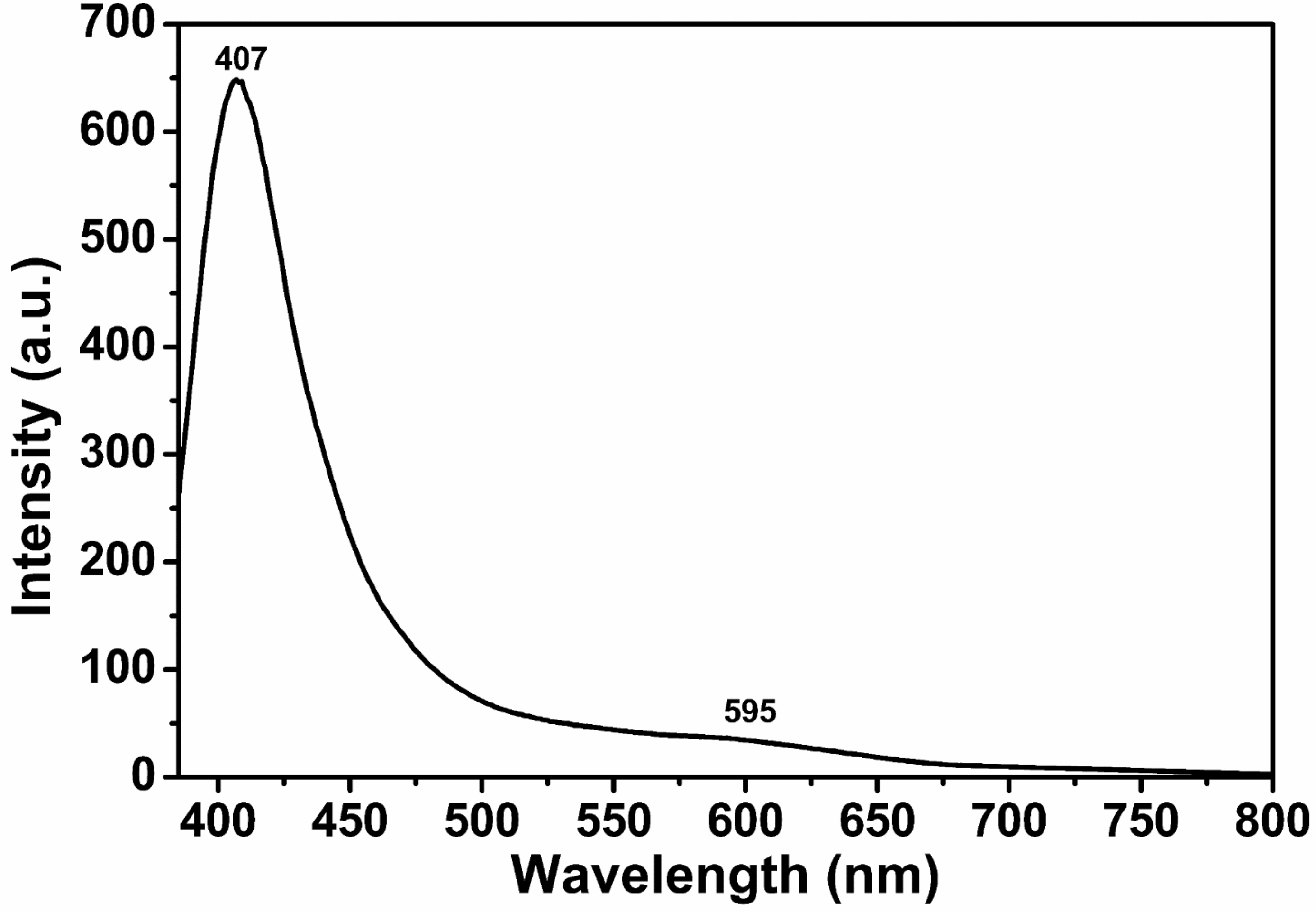

Figure 4.17: Emission spectrum of TNDI in TFA

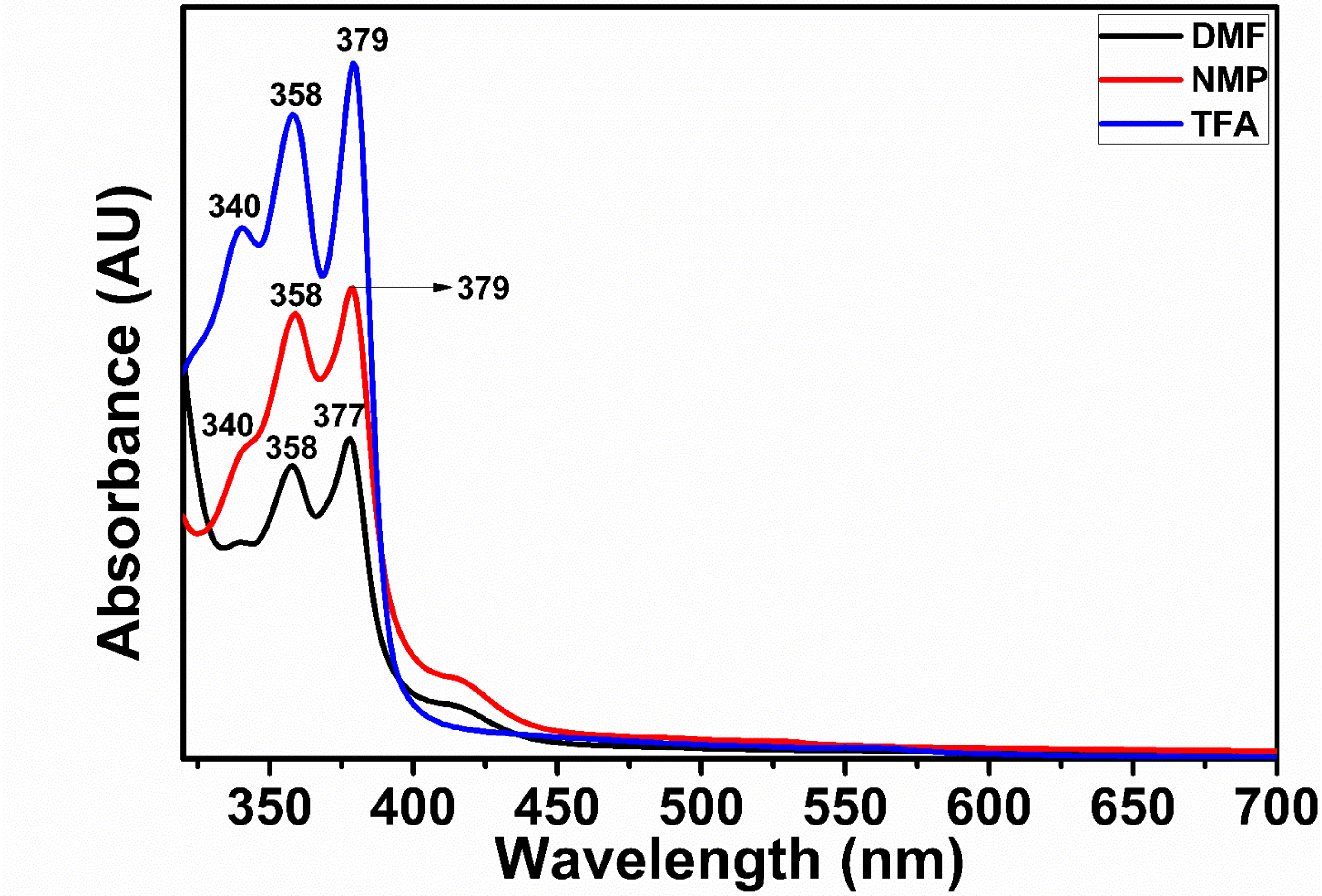

Figure 4.18: Absorption spectra of TNDI in DMF, NMP and TFA

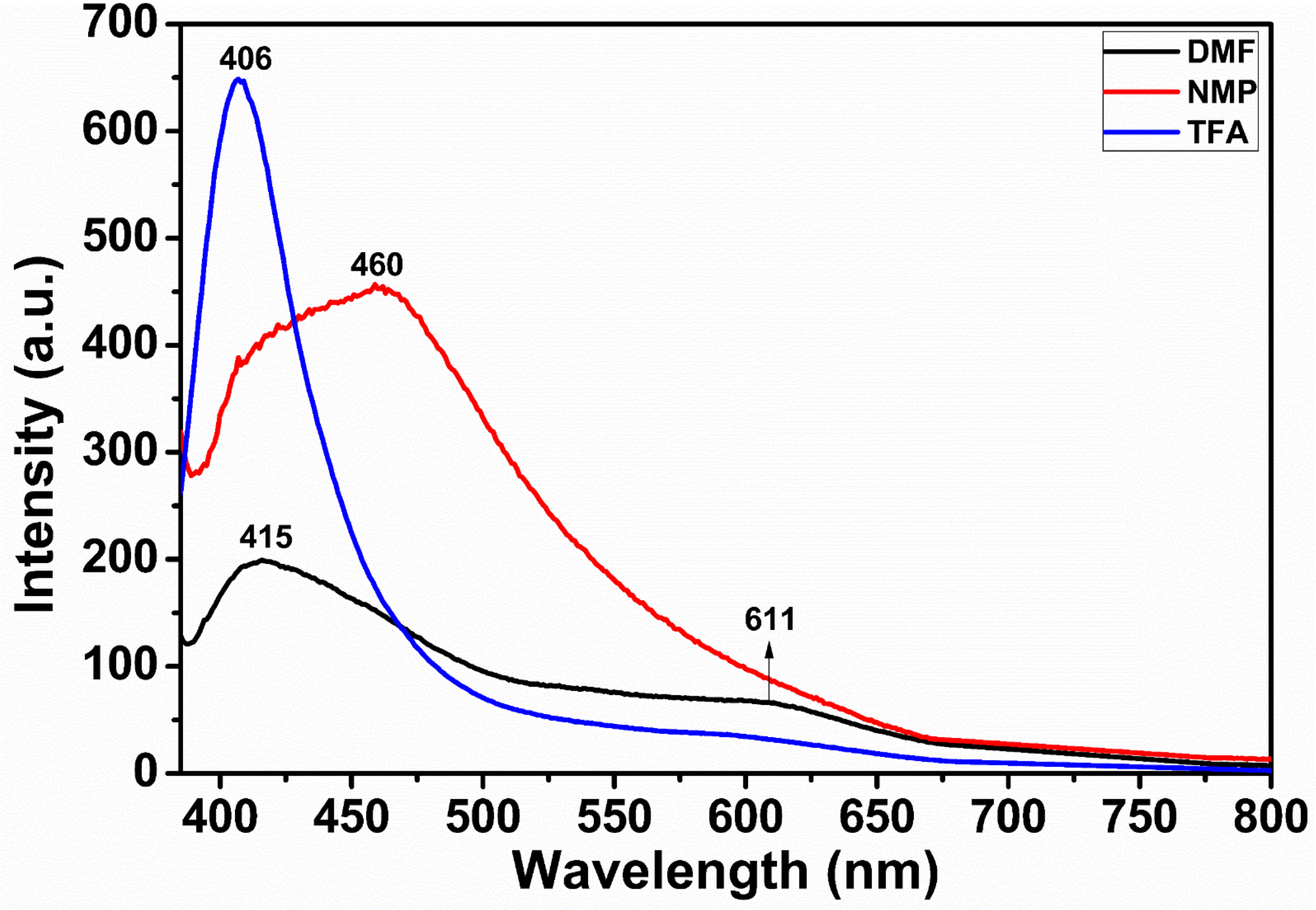

Figure 4.19: Emission spectra of TNDI in DMF, NMP and TFA

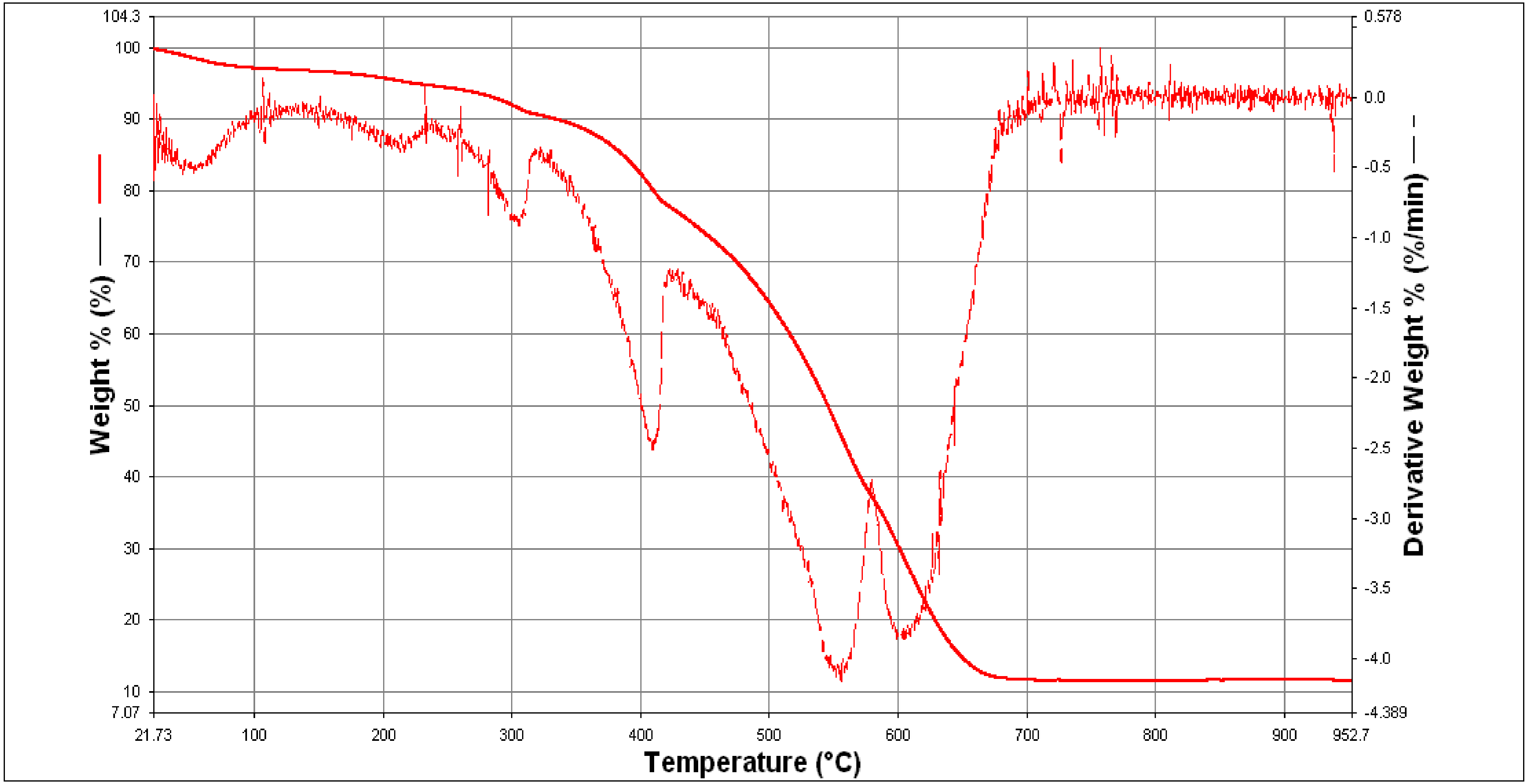

Figure 4.20: TGA thermogeram of TNDI at heating rate of 10 °C/min in oxygen

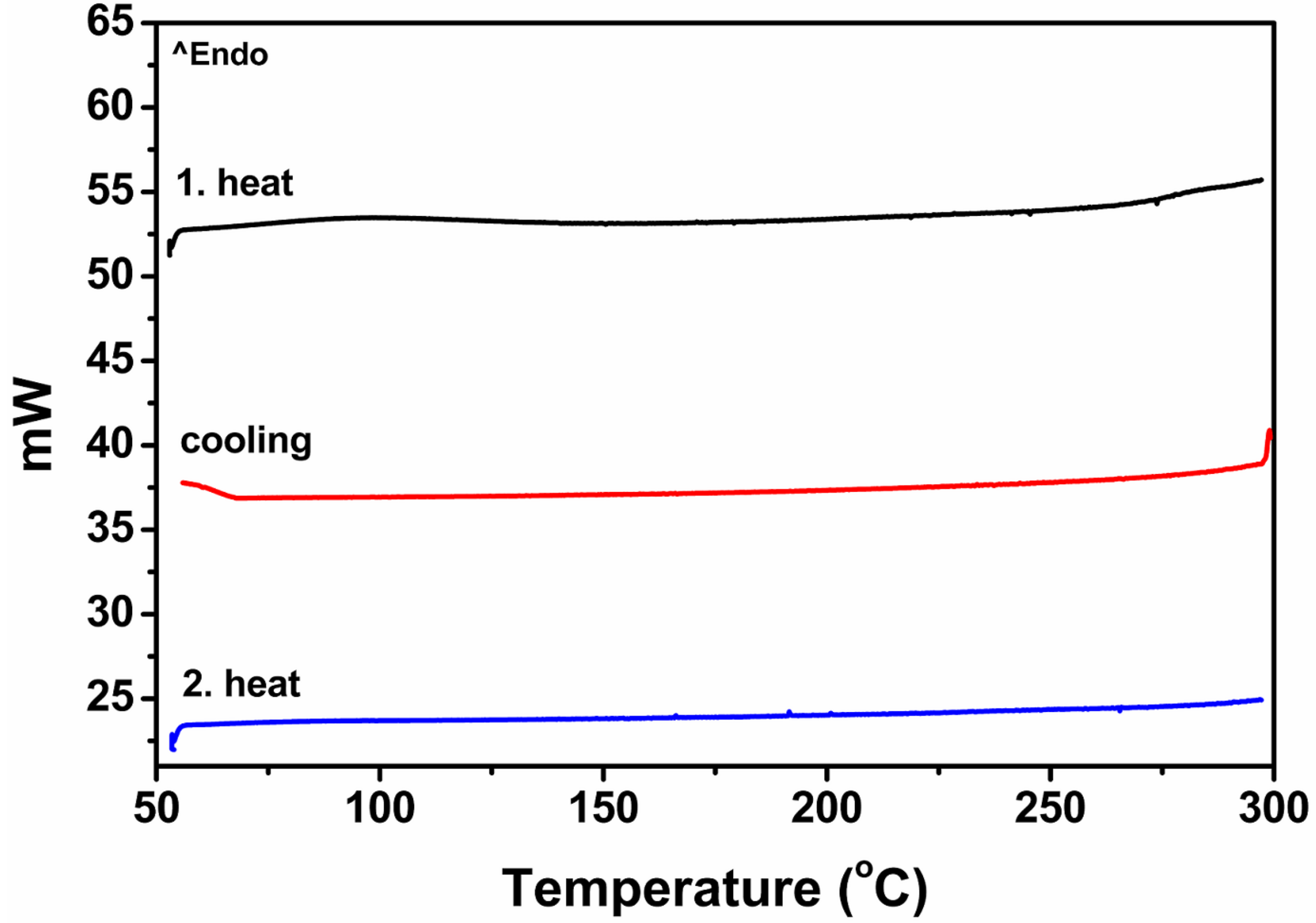

Figure 4.21: DSC thermogeram of TNDI

Table 4.10: Photophysical properties of TNDI

solvent	**λ_{max}(nm)**	**ε_{max}($M^{-1}.cm^{-1}$)**	**$\Delta\bar{\upsilon}_{1/2}$ (cm^{-1})**	**τ_0(ns)**	**K_f(s^{-1})**	**F**	**E_s(kcal mol^{-1})**
TFA	380	110000	625	7.351	1.36×10^8	0.297	75.26
DMF	379	70000	1893.55	3.793	2.63×10^8	0.573	75.46
NMP	360	72700	771.75	8.084	1.23×10^8	0.242	97.44

Chapter 5

RESULTS AND DISCUSSIONS

5.1 Synthesis and Characterization

The synthetic path of TNDI is presented in Scheme 3.1. TNDI was synthesized by condensation of 4,6-diamino-2-pyrimidinethiol with 1,4,5,8,-naphthalenetetracarboxylic dianhydride (NDA) using *m*-cresol/isoquinoline mixture as solvent under argon atmosphere. The synthesized product was characterized by FTIR and elemental analysis. Photophysical properties were determined by UV-vis and emission analysis. Finally, thermal properties were investigated by TGA and DSC techniques.

Solubility is a measure of how a compound dissolves in a solvent. The polarity therefore, of organic compounds is determined by the presence of polar bonds. The solubility of TNDI in various polar protic and polar aprotic solvents are reported in Table 5.1.

Table 5.1: Solubility Properties TNDI in Different Solvents.

Solvents	Solubility	Color
TFA	(+ +)	pale pink
DMF	(+ +)*	light yellow
NMP	(+ +)*	light yellow
DMSO	(- +)	light yellow
DCM	(- +)	light brown
TCE	(- -)	colorless
ACETON	(- -)	colorless
CHL	(- -)	colorless
m-Cresol	(- -)	colorless
Me OH	(- -)	colorless

TFA; Trifluoroacetic acid, DMF; Dimethylformamide, NMP; N-methylpyrrolidinone, DMSO; Dimethyl Sulfoxide, DCM; Dichloromethane, TCE; Trichloroethylene, CHL; Chloroform, Me OH; Methanol, (+ +): Soluble at room temperature, (- +): Partially soluble at room temperature; (- -): Insoluble at room temperature, * Solubility increased upon heating at 60°C.

Complete solubility was observed in polar protic solvent (TFA) at room temperature. In addition to this, TNDI is completely soluble in polar aprotic solvents (NMP, DMF) after heating at 60 °C. In DMSO and DCM, TNDI showed partial solubility.

5.1.1 Analysis of IR Spectra

The FTIR spectrum of TNDI completely represented the functional groups in the synthesized compound. Figure 4.2, 4.3 and 4.4 shows the IR spectra of 4,6-Diamino-2-pyrimidin-thiol, NDA and TNDI respectively.

The FTIR spectrum of NDA (Figure 4.3) shows the following bands: NDA has shown distinct characteristic bands at 3078 cm^{-1}(aromatic C-H stretch), 1780 cm^{-1}(anhydride C=O stretch), 1578, 1517 cm^{-1} (aromatic C=C stretch), 880 cm^{-1}, 760 cm^{-1} , 700 cm^{-1} (C-H bend).

The IR spectrum of 4,6-diamino-2-pyrimidin-thiol (Figure 4.3) shows the following bands: 3438 cm^{-1}, 3393 cm^{-1}, (N-H stretch), 3122 cm^{-1}, 3062 cm^{-1} (aromatic C-H), 1630 cm^{-1} (N-H bending), 1307 cm^{-1} (C-N stretch).

The IR spectrum of T-NDI (Figure 4.4) presents characteristic bands at 3437, 3392 cm^{-1} (N-H stretch); 3190 cm^{-1}, 3130 cm^{-1} (aromatic C-H stretch); 1720 and 1682 cm^{-1} (imide C=O stretch); 1630 cm^{-1} (N-H bending), 1577 cm^{-1} (C=C stretch); 1337cm^{-1} (C-N stretch); and 760 cm^{-1} (C-H bend).

5.2 Absorption and Fluorescence Properties.

The optical and electronic properties of napthalene derivatives are unique and makes napthalene dyes active in it's various application which include optical and photonic materials, machines or devices. These properties are investigated by the absorption spetcurm and emission spectrum of TNDI in polar protic solvents and polar aprotic solvents at (1×10^{-5}M).

5.2.1 Analysis of UV-vis Absorption Spectra of TNDI

Figure 4.6 shows two major characteristic absorption peaks of 4,6-diamino-2-pyrimidinethiol at 352 and 369 nm in DMF.

Figure 4.7 shows three main peaks of NDA in DMF at 330, 347 and 365 nm. These peaks corresponds to the characteristics bands of TNDI for $0\rightarrow0$, $0\rightarrow1$, $0\rightarrow2$ transitions.

Figure 4.8 and 4.9 shows the absorption spectrum of TNDI in DMF before and after microfiltration (0.2 μm SPR), respectively. Three characteristic absorption bans observed at 339, 357, 378 nm and one at 425 nm as a small shoulder. After microfiltration two characteristic absorption bands were observed at 360 and 379 nm and the shoulder one at 425 nm is also observed.

The absorption spectra of TNDI in NMP, before and after microfiltration are shown in Figure 4.10 and 4.11. From Fig 4.10, four absorption peaks are observed at 318, 338, 359, 379 and 415 nm. After microfiltration, two peaks were obderved at 360 nm and 380 nm where the weak peak at 415 nm is almost disappears which indicates aggregation.

Figure 4.12 shows three major characteristic absorption peaks of TNDI in TFA at 338 nm, 358 nm and 380 nm. The three characteristics bans for 0→2, 0→1, and 0→0 peaks represents the π- π electronic transitions aromatic naphthalene.

5.2.2 Analysis of Emission Spectra of TNDI

The emission spectrum of TNDI (Figure 4.13) shows broad excimer like emission at 434 nm and 531 nm in polar aprotic solvent, DMF. After microfiltration as shown in Figure 4.14, slight change occur in spectral shape and emission intensity decreases.

The emission spectra of TNDI in NMP before and after microfiltration are reported in Figure 4.15 and 4.16, respectively. Like in DMF, TNDI shows excimer-like emission spectrum in NMP and peaks observed at 466 nm and 548 nm. Figure 4.16 shows the emission spectrum after microfiltration. Due to lower concentration, the peak at 51-48 nm was disappeared. The broad structure less emission at 461 nm can be attributed due to hydrogen-bonding representing an excimer like emission.

The emission spectrum of TNDI in TFA (Figure 4.17) shows excimer-like emission with one emission peaks at 407 nm due to hydrogen-bonding in polar protic solvent, TFA.

5.3 Thermal Stability

Thermal analysis of TNDI was investigated by differential scanning calorimetry, DSC (10 ^{o}C/min^{-1}) and Thermogravimetry, TGA (5 ^{o}C /min^{-1}) techniques. No glass transition temperature was observed in the DSC run. The curves showed high starting decomposition temperatures (Td) for the compounds. TNDI was stable up to 325 ^{o}C, the compound also showed a rapid weight loss of 9 % between 325 ^{o}C and 420 ^{o}C. When TNDI was heated to 952 ^{o}C, 88% of the initial weight was lost and 12% char yield was left behind. Therefore, TNDI illustrates a good thermal stability.

Chapter 6

CONCLUSION

A new naphthalene diimide dye that contains powerful binding site for metal ions has been successfully synthesized. The synthesized product was characterized by FTIR, UV-vis, emission, DSC, TGA and elemental analysis. The optical and photophysical properties of the compound was investigated in detail by absorption and emission spectroscopy.

The product TNDI was found to be soluble in polar protic solvent TFA at room temperature. In addition, TNDI is also completely soluble in polar aprotic solvents DMF and NMP after heating at 60 ^{o}C.

The compound shows increased absorptions with aggregation and excimer-like emissions. In polar aprotic solvents DMF and NMP, the absorption spectra showed that TNDI has similar properties.

The emission spectra of TNDI showed excimer like emission due to hydrogen bonding between TNDI molecule and also with solvent-dye molecules. The fluorescence quantum yields of TNDI were low and the compound is thermally stable and serves as potentials for photonic technologies.

REFERENCES

[1] Langhals, H. (1995). Cyclic carboxylic imide structures as structure elements of high stability. Novel developments in perylene dye chemistry. *Heterocycles*, *1*(40), 477-500.

[2] Bhosale, S. V., Jani, C. H., & Langford, S. J. (2008). Chemistry of naphthalene diimides. *Chemical Society Reviews*, *37*(2), 331-342.

[3] Suraru, S. L., Burschka, C., & Würthner, F. (2013). Diindole-Annulated Naphthalene Diimides: Synthesis and Optical and Electronic Properties of Syn- and Anti-Isomers. *The Journal of organic chemistry*, *79*(1), 128-139.

[4] Aleshinloye, A. O., Bodapati, J. B., & Icil, H. (2015). Synthesis, characterization, optical and electrochemical properties of a new chiral multichromophoric system based on perylene and naphthalene diimides. *Journal of Photochemistry and Photobiology A: Chemistry*, *300*, 27-37.

[5] Mukhopadhyay, P., Iwashita, Y., Shirakawa, M., Kawano, S. I., Fujita, N., & Shinkai, S. (2006). Spontaneous colorimetric sensing of the positional isomers of dihydroxynaphthalene in a 1D organogel matrix. *Angewandte Chemie*, *118*(10), 1622-1625.

[6] Ozser, M. E., Yucekan, I., Bodapati, J. B., & Icil, H. (2013). New naphthalene polyimide with unusual molar absorption coefficient and excited state properties:

Synthesis, photophysics and electrochemistry. *Journal of Luminescence*, *143*, 542-550.

[7] Bell, T. D., Bhosale, S. V., Forsyth, C. M., Hayne, D., Ghiggino, K. P., Hutchison, J. A., ... & Woodward, C. P. (2010). Melt-induced fluorescent signature in a simple naphthalenediimide. *Chemical Communications*, *46*(27), 4881-4883.

[8] Huang, C., Barlow, S., & Marder, S. R. (2011). Perylene-3, 4, 9, 10-tetracarboxylic acid diimides: Synthesis, physical properties, and use in organic electronics. *The Journal of organic chemistry*, *76*(8), 2386-2407.

[9] Adiga, S. P., & Shukla, D. (2010). Electronic Structure and Charge-Transport Properties of N, N′-Bis (cyclohexyl) naphthalene Diimide. *The Journal of Physical Chemistry C*, *114*(6), 2751-2755.

[10] Asir, S., Demir, A. S., & Icil, H. (2010). The synthesis of novel, unsymmetrically substituted, chiral naphthalene and perylene diimides: Photophysical, electrochemical, chiroptical and intramolecular charge transfer properties. *Dyes and Pigments*, *84*(1), 1-13.

[11] Figueiredo, K. M., Marcon, R. O., Campos, I. B., Nantes, I. L., & Brochsztain, S. (2005). Photoinduced electron transfer between cytochrome c and a novel 1, 4, 5, 8-naphthalenetetracarboxylic diimide with amphiphilic character. *Journal of Photochemistry and Photobiology B: Biology*, *79*(1), 1-9.

[12] Amabilino, D. B., & Stoddart, J. F. (1995). Interlocked and intertwined structures and superstructures. *Chemical reviews, 95*(8), 2725-2828.

[13] Fernando, R., Mao, Z., Muller, E., Ruan, F., & Sauvé, G. (2014). Tuning the organic solar cell performance of acceptor 2, 6-dialkylaminonaphthalene diimides by varying a linker between the imide nitrogen and a thiophene group. *The Journal of Physical Chemistry C*, *118*(7), 3433-3442.

[14] Islam, M. M., Fujii, S., Sato, S., Okauchi, T., & Takenaka, S. (2015). A selective G-quadruplex DNA-stabilizing ligand based on a cyclic naphthalene diimide derivative. *Molecules, 20*(6), 10963-10979.

[15] Pantoş, G. D., Pengo, P., & Sanders, J. K. (2007). Hydrogen-Bonded Helical Organic Nanotubes. *Angewandte Chemie International Edition*, *46*(1-2), 194-197.

[16] Sessler, J. L., Brown, C. T., O'Connor, D., springs, S. L., Wang, R., Sathiosatham, M., & Hirose, T. (1998). *J. Org. Chem*., 63, 7370–7374.

[17] Pantoş, G. D., Pengo, P., & Sanders, J. K. (2007). Hydrogen-Bonded Helical Organic Nanotubes. *Angewandte Chemie International Edition*, *46*(1-2), 194-197.

[18] Das, A., & Ghosh, S. (2014). Stimuli-Responsive Self-Assembly of a Naphthalene Diimide by Orthogonal Hydrogen Bonding and Its Coassembly

with a Pyrene Derivative by a Pseudo-Intramolecular Charge-Transfer Interaction. *Angewandte Chemie International Edition*, *53*(4), 1092-1097.

[19] Das, A., Molla, M. R., Maity, B., Koley, D., & Ghosh, S. (2012). Hydrogen-Bonding Induced Alternate Stacking of Donor (D) and Acceptor (A) Chromophores and their Supramolecular Switching to Segregated States.*Chemistry–A European Journal*, *18*(32), 9849-9859.

[20] Tomasulo, M., Naistat, D. M., White, A. J., Williams, D. J., & Raymo, F. M. (2005). Self-assembly of naphthalene diimides into cylindrical microstructures. *Tetrahedron letters*, *46*(34), 5695-5698.

[21] Pramanik, G. (2010). *Towards Novel Naphthalene Based Near Infrared Dyes for Bioimaging Applications* (Doctoral dissertation, National University of Singapore).

[22] Sakai, N., Mareda, J., Vauthey, E., & Matile, S. (2010). Core-substituted naphthalenediimides. *Chemical Communications*, *46*(24), 4225-4237.

[23] Gudeika, D., Lygaitis, R., Gražulevičius, J. V., Kublickas, R. H., Rubežienė, V., & Vedegytė, J. (2012). Synthesis and properties of dimeric naphthalene diimides. *chemija*, *23*(3), 233-238.

[24] Zhao, X., Ma, L., Zhang, L., Wen, Y., Chen, J., Shuai, Z., & Zhan, X. (2013). An acetylene-containing perylene diimide copolymer for high mobility n-channel transistor in air. *Macromolecules*, *46*(6), 2152-2158.

[25] Guo, X., Kim, F. S., Seger, M. J., Jenekhe, S. A., & Watson, M. D. (2012). Naphthalene diimide-based polymer semiconductors: synthesis, structure–property correlations, and n-channel and ambipolar field-effect transistors. *Chemistry of Materials*, *24*(8), 1434-1442.

[26] Jung, B. J., Tremblay, N. J., Yeh, M. L., & Katz, H. E. (2010). Molecular Design and Synthetic Approaches to Electron-Transporting Organic Transistor Semiconductors†. *Chemistry of Materials*, *23*(3), 568-582.

[27] Chang, C. W., Tsai, H. Y., & Chen, K. Y. (2014). Green perylene bisimide dyes: synthesis, photophysical and electrochemical properties. *Materials*, *7*(8), 5488-5506.

[28] Zhan, X., Facchetti, A., Barlow, S., Marks, T. J., Ratner, M. A., Wasielewski, M. R., & Marder, S. R. (2011). Rylene and related diimides for organic electronics. *Advanced Materials*, *23*(2), 268-284.

[29] Yiseen, G. A. (2014). Synthesis and Characterization of New Monomer and New polymer of Naphthalene diimide: Electrochemical and Optical Studies. *Int. J. Electrochem. Sci*, *9*, 2575-2588.

[30] Kim, M. B., & Dixon, D. W. (2008). Hydrolysis of aliphatic naphthalene diimides: effect of charge placement in the side chains. *Journal of Physical Organic Chemistry*, *21*(9), 731-737.

[31] Suraru, S. L., & Würthner, F. (2014). Strategies for the synthesis of functional naphthalene diimides. *Angewandte Chemie International Edition*, *53*(29), 7428-7448.

[32] Ruland, G E., (1997), PhD Thesis, State University of New York.

[33] Jones, B. A., Facchetti, A., Marks, T. J., & Wasielewski, M. R. (2007). Cyanonaphthalene diimide semiconductors for air-stable, flexible, and optically transparent n-channel field-effect transistors. *Chemistry of materials*, *19*(11), 2703-2705.

[34] Aveline, B. M., Matsugo, S., & Redmond, R. W. (1997). Photochemical mechanisms responsible for the versatile application of naphthalimides and naphthaldiimides in biological systems. *Journal of the American Chemical Society*, *119*(49), 11785-11795.

[35] Grimshaw, J. (2000). *Electrochemical reactions and mechanisms in organic chemistry*. Elsevier.

[36] Schafer, H. J. (2004*). Encyclopedia of Electrochemistry*, Vol. 8, *Organic Electrochemistry*.

[37] Wang, F., Tang, J., Liu, J., Wang, Y., Wang, R., Niu, L., & Huang, Z. (2011). Highly Efficient Photoinduced Electron Transfer in a Novel Tetrakis (tetraphenylporphyrinatozinc)/Perylenetetracarboxidiimide Array and Its

Application to a Photovoltaic Device. *Bulletin of the Chemical Society of Japan*, *84*(4), 427-436.

[38] Dadashi-Silab, S., Doran, S., & Yagci, Y. (2016). Photoinduced Electron Transfer Reactions for Macromolecular Syntheses. *Chemical reviews*.

[39] Wielopolski, M. (2010). Motivation—Focusing on Molecular Wires. In *Testing Molecular Wires* (pp. 9-10). Springer Berlin Heidelberg.